

DPB-splines: The Decoupled Basis of Patchwork Splines

Nora Engleitner and Bert Jüttler

Abstract We consider partitions of the d -dimensional unit cube into patches with an associated tensor-product spline space for each of them. The spline spaces possess the same multi-degree $\mathbf{p} = (p_1, \dots, p_d)$ and the same maximum smoothness $C^{\mathbf{p}-1}$, but the choice of the knots is very flexible. Under certain assumptions, we show how to construct Decoupled Patchwork B-splines (DPB-splines) that span the corresponding patchwork spline space \mathbb{P} . More precisely, we generate a basis for the space \mathbb{P} formed by all $C^{\mathbf{p}-1}$ smooth functions that admit patch-wise representations in the associated spline spaces. Based on the framework of decoupled tensor-product B-splines [31, 32], we obtain a basis that is algebraically complete, forms a convex partition of unity, and preserves the coefficients of the local B-spline representations. Furthermore, we present an adaptive refinement algorithm for surface approximation generating partitions that satisfy the required assumptions and hence can be equipped with a DPB-spline basis.

1 Introduction

Tensor-product B-splines, which are the standard for describing free-form geometries in Computer-Aided Design [14] possess a fundamental limitation: Their tensor-product structure does not support local refinement. Therefore, adaptive spline constructions have been developed in order to overcome this restriction and provide more flexibility in design and analysis. Forsey and Bartels were the first to introduce hierarchical B-spline refinement [15]. Their hierarchical construction was extended by Kraft, who established a selection mechanism that defines a basis for the hierarchical spline space [27].

Nora Engleitner and Bert Jüttler
Institute of Applied Geometry, Johannes Kepler University, Linz, e-mail:
bert.juettler@jku.at

T-splines [35] have been developed as an adaptive construction on meshes with T-joints. In general these splines are not linearly independent and therefore, analysis-suitable (AS) T-splines and AS++ T-splines have been introduced and discussed in [8, 30, 33, 41]. Moreover, polynomial splines over hierarchical T-meshes [25, 29] and locally refined B-splines [9] have been established. Recently, the latter construction has been generalized to LR T-splines [7], where local refinement is performed on an initial T-mesh instead of a tensor-product mesh.

In order to restore the partition of unity property for hierarchical splines, a truncation mechanism has been introduced in [18]. The resulting truncated hierarchical B-splines (THB-splines) possess good mathematical properties, see [19, 21, 32, 36, 38] for a detailed analysis of stability, completeness and approximation power. Applications of (T)HB-splines include surface approximation [4, 22, 26] and isogeometric analysis [1, 2, 3, 5, 28, 34]. Aspects of the implementation have been discussed in [16, 17]. Moreover, the hierarchical principle has been applied to other constructions, such as Powell-Sabin splines [37], triangular splines [40], box splines [20, 23, 42], B-splines on triangulations [24], T-splines [6, 13], and subdivision functions [39, 43].

While THB-splines possess good mathematical properties, they are not as flexible as other constructions like T-splines or LR B-splines. Hierarchical B-splines rely on a sequence of *nested* spline spaces and therefore, the choice of possible refinement strategies is limited. Recently, we generalized hierarchical splines to Patchwork B-splines (PB-splines), which are defined on a sequence of partially nested spline spaces and enable the use of independent refinement strategies in different parts of the domain [10, 12]. An adapted version of Kraft's selection mechanism generates a basis for the patchwork spline space under certain assumptions. Similar to the hierarchical splines, a truncation mechanism has been established in order to obtain the basis of truncated PB-splines (TPB-splines) [10] that forms a non-negative partition of unity. Applications of the PB-splines in surface approximation and to lofting B-spline curves [11] have shown the potential of this new construction.

Although the (T)PB-splines provide increased flexibility, there are still certain limitations on the available refinement strategies. For instance, a region that separates two coarser spline spaces is required to have a certain degree-dependent width, see Fig. 1, bottom row. Additionally, the spaces that are present in a degree-dependent neighborhood of any cell need to be (upwards or downwards) compatible with the chosen space for this cell if TPB-splines are to be generated. Consequently, a region that separates two finer (but non-nested) refinement regions is also required to possess a certain degree-dependent width, see Fig. 1, top row. For instance, also the PB-spline hierarchies considered in [11] for solving the lofting problem are not suitable for TPB-splines.

Finally we note that (T)PB-splines are not algebraically complete in general. This is similar to THB-splines, see [31], where the use of decoupled B-splines has led to significant improvements in this regard. We build on this

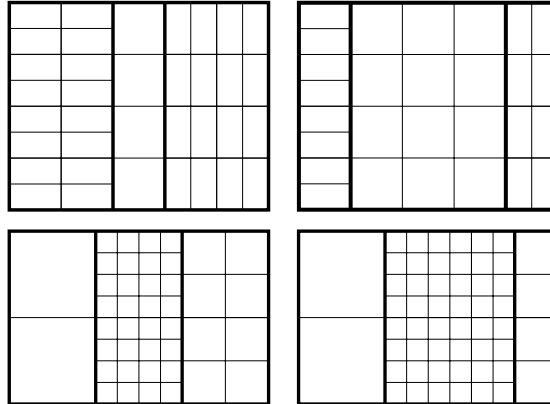


Fig. 1: Invalid (left) and valid (right) meshes for bicubic PB-splines (bottom) and TPB-splines (top).

idea to define the new framework of *Decoupled Patchwork B-splines* (DPB-splines). More precisely, we define local basis functions, called patch B-splines, that are obtained by restricting and decoupling tensor-product B-splines.

The remainder of this paper is organized as follows: Section 2 introduces the general framework consisting of patches, the local spline spaces and a patchwork spline space. Moreover, we observe that the patchwork spline space is equal to the full spline space, i.e., a basis for this space is algebraically complete. A truncation and selection mechanism are then used to define the DPB-splines in Section 3. We identify assumptions that are needed in order to guarantee a certain order of smoothness of the basis functions and for characterizing the obtained spline space. These assumptions affect only a patch and its neighbors. The mathematical properties of the DPB-splines are analyzed in Section 4. In particular, the basis functions possess continuous values and derivatives up to a certain order, they span the patchwork spline space and form a convex partition of unity. Furthermore, we identify a simple sufficient condition for a certain class of patches that guarantees that the assumptions are satisfied. Section 5 provides several examples that compare the flexibility of DPB-splines with TPB- and THB-splines. We introduce an improved refinement algorithm for least-squares fitting in Section 7, which generates hierarchies that can be equipped with a Decoupled Patchwork and a (truncated) Patchwork B-spline basis. Two examples are used to illustrate the advantages of this new strategy. Finally, we conclude the paper.

2 The patchwork hierarchy

For constructing DPB-splines we generate a hierarchy consisting of patches and corresponding spaces, which are not necessarily nested. Furthermore, the collection of patches and spline spaces allows the definition of a patchwork spline space.

2.1 Patches

We consider a finite sequence of *patches* $\{\pi^\ell\}_{\ell=1,\dots,N}$, which are closed subsets of the d -dimensional unit cube $[0, 1]^d$. The upper index ℓ will be called the *level*. The patches possess a mutually disjoint interior, $\text{int}(\pi^\ell) \cap \text{int}(\pi^k) = \emptyset$, for $k \neq \ell$, and their union defines the *domain*,

$$\Omega = \bigcup_{\ell=1}^N \pi^\ell.$$

Not only the entire domain but certain subsets thereof will be used in the remainder of the paper. An index set $\mathcal{D} \subseteq \{1, \dots, N\}$ generates the *subdomain*,

$$\Delta_{\mathcal{D}} = \bigcup_{\ell \in \mathcal{D}} \pi^\ell \subseteq \Omega. \quad (1)$$

In particular, we define $\Delta_{\mathcal{D}, \geq \ell} = \Delta_{\mathcal{D}} \cap \Delta_{\geq \ell}$, with the index set $\geq \ell = \{\ell, \dots, N\}$, as the subdomain formed by all patches in $\Delta_{\mathcal{D}}$ with level greater or equal to ℓ . Furthermore, we introduce the neighboring index set

$$\mathcal{N}^\ell = \{k : k > \ell \text{ and } \pi^k \cap \pi^\ell \neq \emptyset\},$$

that comprises the levels $k > \ell$ of higher level neighboring patches of π^ℓ . The index set of higher level neighboring patches in $\Delta_{\mathcal{D}}$ will be denoted as

$$\mathcal{N}_{\mathcal{D}}^\ell = \mathcal{N}^\ell \cap \mathcal{D}.$$

The two index sets \mathcal{N}^ℓ and $\mathcal{N}_{\mathcal{D}}^\ell$ define the subdomains $\Delta_{\mathcal{N}^\ell}$ and $\Delta_{\mathcal{N}_{\mathcal{D}}^\ell}$, respectively.

Example 1 We consider the subdivision of the unit square into six patches, π^1, \dots, π^6 . Note that the patches might possess several connected components, as it is the case for patch π^2 in this example. Fig. 2 depicts several subdomains of Ω . The subdomain $\Delta_{\geq 3}$ is formed by the patches π^3, \dots, π^6 as illustrated in Fig. 2a. Consider $\mathcal{D} = \{2, 4, 5\}$, thus $\Delta_{\mathcal{D}, \geq 3} = \pi^4 \cup \pi^5$, see Fig. 2b. The higher level neighbors of π^3 define the index set $\mathcal{N}^3 = \{4, 6\}$, see

Fig. 2c. The intersection of $\Delta_{\mathcal{N}^3}$ and $\Delta_{\mathcal{D}}$ gives the subdomain $\Delta_{\mathcal{N}^3_{\mathcal{D}}}$, which consists of π^4 , see Fig. 2d. \diamond

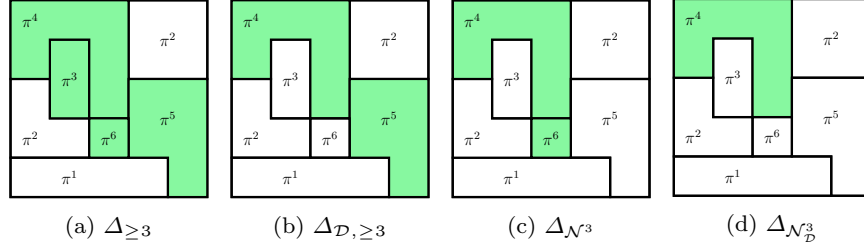


Fig. 2: Example 1 – Various subdomains for $\mathcal{D} = \{2, 4, 5\}$.

Except for trivial situations, each patch shares parts of its boundary $\partial\pi^\ell$ with patches of a different level. The part of the boundary that intersects with patches of a *higher* level will be called the *constraining boundary*,

$$\Gamma^\ell = \Delta_{\geq \ell+1} \cap \pi^\ell.$$

In addition we define the constraining boundary

$$\Gamma_{\mathcal{D}}^\ell = \Gamma^\ell \cap \Delta_{\mathcal{D}} = \Delta_{\mathcal{D}, \geq \ell+1} \cap \pi^\ell,$$

with respect to the subdomain $\Delta_{\mathcal{D}}$.

Example 2 We re-visit the previous example. Fig. 3 shows the constraining boundaries Γ^4 , $\Gamma_{\mathcal{D}}^4$, $\Gamma_{\mathcal{N}^3}^4$ and $\Gamma_{\mathcal{N}^3_{\mathcal{D}}}^4 = \emptyset$. \diamond

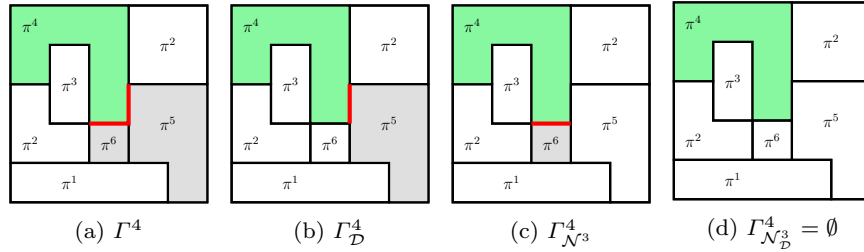


Fig. 3: Example 2 – Various constraining boundaries (shown in red).

2.2 Spline spaces

For each level ℓ , we choose a globally¹ defined tensor-product spline basis \hat{B}^ℓ that consists of individual basis functions $\hat{\beta}^\ell \in \hat{B}^\ell$, spanning a certain spline space \hat{V}^ℓ . Note that we consider sets \hat{B}^ℓ of basis functions and use the symbol $\hat{\beta}^\ell$ to represent their elements. The upper index indicates the level but does not identify individual basis functions.

More precisely, the basis functions are tensor-product B-splines of degree $\mathbf{p} = (p_1, \dots, p_d)$ defined on d open knot vectors with $(p_i + 1)$ -fold boundary knots 0 and 1 for $i = 1, \dots, d$. All inner knots possess multiplicity 1. Hence, we obtain B-splines of maximal smoothness, $C^{\mathbf{s}}(\Omega)$, with $\mathbf{s} = \mathbf{p} - \mathbf{1}$. In other words, the basis functions possess continuous values and partial derivatives up to order $p_i - 1$ in each variable x_i separately. The supports² of the functions $\hat{\beta}^\ell$ are axis-aligned open boxes in $[0, 1]^d$.

In addition to the B-spline bases, which are independent of the patches π^ℓ , we define *local* spline bases B^ℓ on π^ℓ that consist of *patch B-splines* β^ℓ and span the spaces V^ℓ . The basis functions are constructed by *decoupling* the restricted function $\hat{\beta}^\ell|_{\pi^\ell}$, see [31]. More precisely, for each connected component ϕ of $\text{supp}\hat{\beta}^\ell \cap \pi^\ell$ we obtain a basis function

$$\beta^\ell = \begin{cases} \hat{\beta}^\ell & \text{on } \phi \\ 0 & \text{on } \pi^\ell \setminus \phi. \end{cases} \quad (2)$$

The knot hyperplanes of the space V^ℓ divide the patch π^ℓ into cells $z \in Z^\ell$, where Z^ℓ denotes the set of all cells of level ℓ .

For later reference we note that

$$\text{supp}\beta^k \cap \Gamma^\ell = \text{supp}\beta^k \cap \Gamma_{\mathcal{D}}^\ell, \quad (3)$$

for $\beta^k \in B^k$ and any index set \mathcal{D} with $k \in \mathcal{D}$ and $\ell < k$.

Example 3 We consider three different biquadratic tensor-product B-splines $\hat{\beta}^\ell$ and discuss the resulting patch B-splines with respect to a U-shaped patch π^ℓ , represented as gray area in Fig. 4. The knot vectors of level ℓ define the grid that is illustrated in the three pictures. The supports of the B-splines are depicted as blue squares, and the blue circles indicate their Greville points. Depending on the location of the support with respect to the patch we obtain zero, one or two patch B-splines. \diamond

The functions in B^ℓ possess good mathematical properties on π^ℓ : They are linearly independent, non-negative, form a partition of unity and have continuous values and partial derivatives up to order $p_i - 1$ in each variable x_i .

¹ i.e., with domain $[0, 1]^d$.

² Note that we use the set-theoretic definition of the support, i.e., for a function $f : \Omega \mapsto \mathbb{R}^d$ the support of f is defined as $\text{supp}f = \{\mathbf{x} \in \Omega : f(\mathbf{x}) \neq 0\}$.

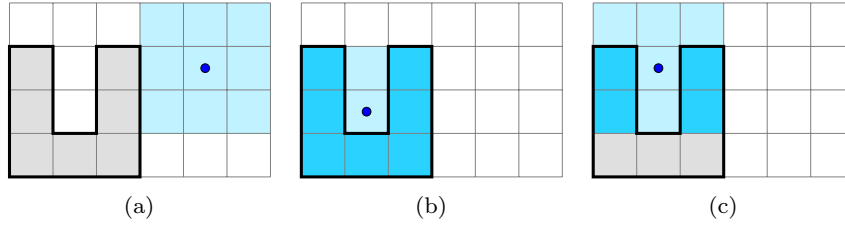


Fig. 4: Example 3 – Restriction of three tensor-product B-splines to a U-shaped patch.

2.3 The patchwork spline space

We conclude this section by introducing the *patchwork spline space*. On a general subdomain $\Delta_{\mathcal{D}}$ we define

$$\mathbb{P}_{\mathcal{D}} = \{f \in C^s(\Delta_{\mathcal{D}}) : f|_{\pi^k} \in \mathbb{V}^k, \text{ for } k \in \mathcal{D}\}.$$

Note that the tensor-product polynomials of degree \mathbf{p} restricted to the subdomain $\Delta_{\mathcal{D}}$ are contained in the patchwork spline space $\mathbb{P}_{\mathcal{D}}$. With $\mathbb{P}_{\mathcal{D}, \geq \ell}$ we denote the patchwork spline space on the subdomain $\Delta_{\mathcal{D}, \geq \ell}$, while $\mathbb{P} = \mathbb{P}_{\geq 1}$ is the patchwork spline space on the entire domain.

In addition to the patchwork spline space $\mathbb{P}_{\mathcal{D}}$ we consider the full spline space

$$\mathbb{F}_{\mathcal{D}} = \{f \in C^s(\Delta_{\mathcal{D}}) : f|_z \in \mathbb{I}^{\mathbf{p}} \quad \forall z \in Z^{\ell}, \ell \in \mathcal{D}\},$$

where $\mathbb{I}^{\mathbf{p}}$ is the space of tensor-product polynomials of degree \mathbf{p} . We obtain the following result:

Corollary 1 *The patchwork spline space $\mathbb{P}_{\mathcal{D}}$ is equivalent to the full spline space $\mathbb{F}_{\mathcal{D}}$.*

Proof Theorem 2.12. of [32] implies that $\mathbb{P}_{\mathcal{D}} = \mathbb{F}_{\mathcal{D}}$. \square

Thus, a basis that spans the patchwork spline spaces is *algebraically complete*.

3 Decoupled Patchwork B-splines

We define a basis for the patchwork spline space by suitably adapting Kraft's selection mechanism [27] to the patch structure.

3.1 Preliminaries

Our construction is based on the natural assumption that the spline spaces associated with neighboring patches are nested.

Assumption NNC – Nested Neighbor Condition

Any two globally defined spline spaces satisfy $\hat{\mathbb{V}}^\ell \subseteq \hat{\mathbb{V}}^k$ if $k \in \mathcal{N}^\ell$.

We introduce the *extension operator*, $\mathcal{E} : B^\ell \mapsto \hat{B}^\ell$, that transforms a patch B-spline $\beta^\ell \in B^\ell$ into the globally defined tensor-product B-spline $\mathcal{E}(\beta^\ell) = \hat{\beta}^\ell \in \hat{B}^\ell$ such that

$$\beta^\ell = \hat{\beta}^\ell|_{\text{supp}\beta^\ell}. \quad (4)$$

The extension of a patch B-spline β^ℓ is always denoted by $\hat{\beta}^\ell$ in the remainder of this paper. Note that different patch B-splines β^ℓ and β'^ℓ with disjoint supports possess the same extension $\hat{\beta}^\ell = \hat{\beta}'^\ell$ if they are derived from the same tensor-product B-spline. It follows that $\hat{\beta}^\ell|_{\pi^\ell} \in \mathbb{V}^\ell$ since

$$\hat{\beta}^\ell|_{\pi^\ell} = \sum_{\substack{\beta'^\ell \in B^\ell \\ \hat{\beta}'^\ell = \hat{\beta}^\ell}} \beta'^\ell.$$

The dual functionals that generate the coefficients of the local representation

$$f(\mathbf{x}) = \sum_{\beta^\ell \in B^\ell} \lambda_{\beta^\ell}(f) \beta^\ell(\mathbf{x}), \quad \text{for } \mathbf{x} \in \pi^\ell,$$

of a function $f \in \mathbb{V}^\ell$ will be denoted by $\lambda_{\beta^\ell}(\cdot)$. If the spaces spanned by a pair of spline bases \hat{B}^ℓ and \hat{B}^k are nested, i.e., $\hat{\mathbb{V}}^\ell \subseteq \hat{\mathbb{V}}^k$, for $\ell < k$, then it holds that $\hat{\beta}^\ell|_{\pi^k} \in \mathbb{V}^k$ and

$$\lambda_{\beta^k}(\hat{\beta}^\ell) = \lambda_{\hat{\beta}^k}(\hat{\beta}^\ell), \quad (5)$$

where the values $\lambda_{\hat{\beta}^k}(\hat{\beta}^\ell)$ of the dual functionals are the coefficients obtained by B-spline refinement.

3.2 Recursive selection

On the subdomain $\Delta_{\mathcal{D}}$ the *Decoupled Patchwork B-splines* $P_{\mathcal{D}}$ are computed recursively, starting at the highest level N and using the initialization $P_{\mathcal{D}}^{N+1} = \emptyset$. Since the index set \mathcal{D} does not necessarily contain all levels, we

distinguish between two cases: When proceeding to the next lower level ℓ , the DPB-splines remain unchanged if $\ell \notin \mathcal{D}$. Otherwise, we *select* functions of levels higher than ℓ that vanish on the constraining boundary,

$$S_{\mathcal{D}}^{\ell+1} = \{\tilde{\beta}_{\mathcal{D}}^k \in P_{\mathcal{D}}^{\ell+1} : \tilde{\beta}_{\mathcal{D}}^k = 0 \text{ on } \Gamma_{\mathcal{D}}^{\ell}\},$$

and apply *truncation* – indicated by the tilde operator – to the extensions of the patch B-splines of level ℓ ,

$$T_{\mathcal{D}}^{\ell} = \{\tilde{\beta}_{\mathcal{D}}^{\ell} : \beta^{\ell} \in B^{\ell}\}.$$

The DPB-splines of level ℓ are then defined as the union of *selected* and *truncated* patch B-splines,

$$P_{\mathcal{D}}^{\ell} = \begin{cases} S_{\mathcal{D}}^{\ell+1} \cup T_{\mathcal{D}}^{\ell} & \text{if } \ell \in \mathcal{D} \\ P_{\mathcal{D}}^{\ell+1} & \text{otherwise.} \end{cases}$$

Since truncation is applied to the extension of the patch B-splines, it extends them to the full domain. More precisely, the *truncated patch B-splines* $\tilde{\beta}_{\mathcal{D}}^{\ell}$, for $\ell \in \mathcal{D}$, are equal to the patch B-splines on π^{ℓ} and extend smoothly (as we shall see later) into $\Delta_{\mathcal{D}, \geq \ell} \setminus \pi^{\ell}$,

$$\tilde{\beta}_{\mathcal{D}}^{\ell} = \begin{cases} \beta^{\ell} & \text{on } \pi^{\ell} \\ \sum_{\substack{\tilde{\beta}_{\mathcal{D}}^k \in P_{\mathcal{D}}^{\ell+1} \\ \text{supp } \beta^{\ell} \cap \text{supp } \beta^k \neq \emptyset}} \lambda_{\beta^k}(\hat{\beta}^{\ell}) \tilde{\beta}_{\mathcal{D}}^k & \text{on } \Delta_{\mathcal{D}, \geq \ell} \setminus \pi^{\ell} \\ 0 & \text{elsewhere.} \end{cases} \quad (6)$$

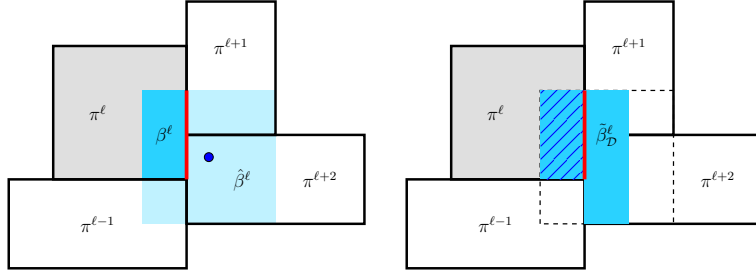


Fig. 5: Left: The supports of a patch B-spline β^{ℓ} (blue) and its extension $\hat{\beta}^{\ell}$ (light blue). Right: The support (blue) of the corresponding truncated patch B-spline $\tilde{\beta}_{\mathcal{D}}^{\ell}$. In the hatched area, it is equal to the patch B-spline and it is smoothly extended in the non-hatched part.

The support condition $\text{supp}\beta^\ell \cap \text{supp}\beta^k \neq \emptyset$ implies that the truncated functions are linear combinations of non-selected basis functions of higher levels on $\Delta_{\mathcal{D}, \geq \ell} \setminus \pi^\ell$, i.e., of basis functions that do not vanish on the constraining boundary $\Gamma_{\mathcal{D}}^\ell$, see Fig. 5. Note that the sum in (6) considers only basis functions of patches π^k , with $k > \ell$, that are neighbors of π^ℓ , i.e., $k \in \mathcal{N}^\ell \cap \mathcal{D}$. According to NNC it follows that $\hat{\beta}^\ell|_{\pi^k} \in \mathbb{V}^k$ and therefore, the coefficients $\lambda_{\beta^k}(\hat{\beta}^\ell)$ exist and are non-negative due to the properties of B-spline refinement, see Eq. (6).

After completing the recursion we obtain $P_{\mathcal{D}} = P_{\mathcal{D}}^1$ and $P = P_{\geq 1}$.

Lemma 1 *The truncated patch B-splines $\tilde{\beta}_{\mathcal{D}}^k \in T_{\mathcal{D}}^k$ satisfy*

$$\text{supp}\tilde{\beta}_{\mathcal{D}}^k \subseteq \text{supp}\hat{\beta}^k. \quad (7)$$

Proof We prove this statement by induction starting from level $n = \max \mathcal{D}$, which is decreased until we arrive at $n = 1$. According to the piecewise definition of $\tilde{\beta}_{\mathcal{D}}^n$ it follows immediately that

$$\text{supp}\tilde{\beta}_{\mathcal{D}}^n = \text{supp}\beta^n \subseteq \text{supp}\hat{\beta}^n.$$

Now we assume that (7) is satisfied for $k \geq \bar{k} \in \mathcal{D}$ and it remains to be shown that the statement holds as well for $\ell = \max\{m \in \mathcal{D} : m < \bar{k}\}$. We consider a basis function $\tilde{\beta}_{\mathcal{D}}^\ell \in T_{\mathcal{D}}^\ell$. Note that

$$\begin{aligned} & \{\tilde{\beta}_{\mathcal{D}}^k \in P_{\mathcal{D}}^{\ell+1} : \text{supp}\beta^k \cap \text{supp}\beta^\ell \neq \emptyset\} \\ & \subseteq \{\tilde{\beta}_{\mathcal{D}}^k \in T_{\mathcal{D}}^k : \ell < k \in \mathcal{D} \wedge \text{supp}\beta^k \cap \text{supp}\beta^\ell \neq \emptyset\}. \end{aligned}$$

Thus, it follows from the definition of $\tilde{\beta}_{\mathcal{D}}^\ell$ and the induction hypothesis that

$$\text{supp}\tilde{\beta}_{\mathcal{D}}^\ell \subseteq \text{supp}\beta^\ell \cup \left(\bigcup_{k \in \mathcal{D}, k > \ell} \bigcup_{\substack{\beta^k \in B^k \\ \text{supp}\beta^k \cap \text{supp}\beta^\ell \neq \emptyset \\ \lambda_{\beta^k}(\hat{\beta}^\ell) \neq 0}} \text{supp}\hat{\beta}^k \right), \quad (8)$$

where the coefficients $\lambda_{\beta^k}(\hat{\beta}^\ell)$ exist according to NNC. For non-zero coefficients $\lambda_{\beta^k}(\hat{\beta}^\ell) = \lambda_{\beta^k}(\hat{\beta}^\ell) \neq 0$ it holds that the supports of $\hat{\beta}^k$ and $\hat{\beta}^\ell$ are nested, i.e., $\text{supp}\hat{\beta}^k \subseteq \text{supp}\hat{\beta}^\ell$. Therefore, the supports of the B-splines $\hat{\beta}^k$ in (8) are contained in the support of $\hat{\beta}^\ell$. Since also $\text{supp}\beta^\ell \subseteq \text{supp}\hat{\beta}^\ell$ we conclude that $\text{supp}\tilde{\beta}_{\mathcal{D}}^\ell \subseteq \text{supp}\hat{\beta}^\ell$. \square

4 Properties of DPB-splines

Besides NNC, we impose two further assumptions in order to ensure good mathematical properties of the DPB-splines.

4.1 Assumptions and main result

First, we introduce a condition that concerns the intersection of a patch B-spline with the constraining boundaries of lower level patches. To be more precise, if a patch B-spline $\beta^n \in B^n$ does not vanish on a pair of constraining boundaries Γ^ℓ and Γ^k , where $\ell < n$ and $k < n$, then a non-empty intersection of the patch B-spline and the two constraining boundaries is assumed to exist, see also Fig. 6.

Assumption IPC – Intermediate Patch Condition

If $\beta^n \in B^n$ satisfies

$$\text{supp}\beta^n \cap \Gamma^\ell \neq \emptyset, \ell < n \text{ and } \text{supp}\beta^n \cap \Gamma^k \neq \emptyset, k < n,$$

then

$$\text{supp}\beta^n \cap \Gamma^\ell \cap \Gamma^k \neq \emptyset.$$

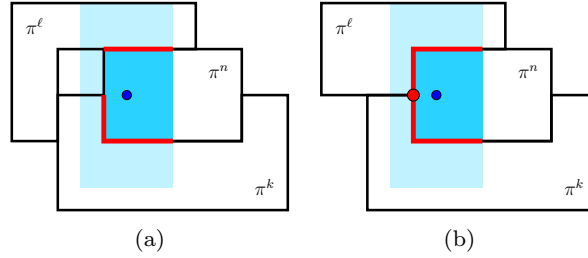


Fig. 6: Intersections (red) of a patch B-spline's support (dark blue) with Γ^ℓ and Γ^k . The support of the associated extension $\hat{\beta}^n$ is also shown (light blue). IPC is violated in (a) and satisfied in (b).

The second assumption is needed to guarantee that the truncated basis functions are C^s -smooth. We impose a condition on the intersection of a patch B-spline with a lower level constraining boundary, see Fig. 7.

Assumption SIC – Support Intersection Condition

The support of a patch B-spline $\beta^n \in B^n$ intersected with a constraining boundary Γ^ℓ ,

$$\text{supp}\beta^n \cap \Gamma^\ell,$$

where $\ell < n$, is connected.

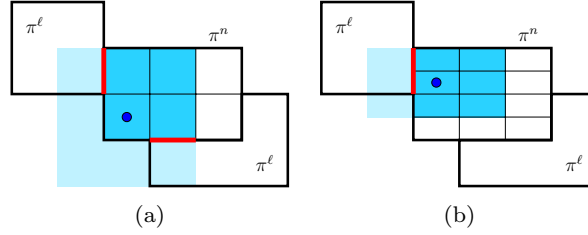


Fig. 7: Intersections (red) of a patch B-spline's support (dark blue) with a constraining boundary Γ^ℓ , $\ell < n$. SIC is violated in (a) and satisfied in (b).

The following theorem shows that the DPB-splines form a basis and characterizes the space that is spanned by them.

Theorem 1 *Assume NNC, IPC and SIC are satisfied. We consider DPB-splines $P_{\mathcal{D}}$ on any subdomain $\Delta_{\mathcal{D}} \subseteq \Omega$.*

- (i) *The functions $\tilde{\beta}_{\mathcal{D}}^\ell \in P_{\mathcal{D}}$ possess continuous values and partial derivatives up to order $p - 1$ in each variable separately.*
- (ii) *The DPB-splines form a basis of the patchwork spline space $\mathbb{P}_{\mathcal{D}}$.*
- (iii) *The DPB-splines satisfy the coefficient preservation property, i.e., for any function $f \in \mathbb{P}_{\mathcal{D}}$ it holds that*

$$f = \sum_{\tilde{\beta}_{\mathcal{D}}^k \in P_{\mathcal{D}}} \lambda_{\beta^k}(f) \tilde{\beta}_{\mathcal{D}}^k, \quad \text{on } \Delta_{\mathcal{D}}. \quad (9)$$

- (iv) *The DPB-spline functions are non-negative and form a partition of unity.*

The proof of this theorem together with several technical lemmas is presented in the next section. Readers not interested in the details of the proof may skip this section and continue directly with Section 5 on page 23.

4.2 Proof of Theorem 1

In the following we assume that NNC, IPC and SIC are always satisfied. Eq. (3) implies that IPC and SIC are then also fulfilled for constraining boundaries $\Gamma_{\mathcal{D}}^\ell$ with respect to index sets \mathcal{D} , see (1).

4.2.1 Some preliminary observations

The proof of Theorem 1 relies on several technical results, see Fig. 8. The first observation will help us to analyze the truncation defined in (6).

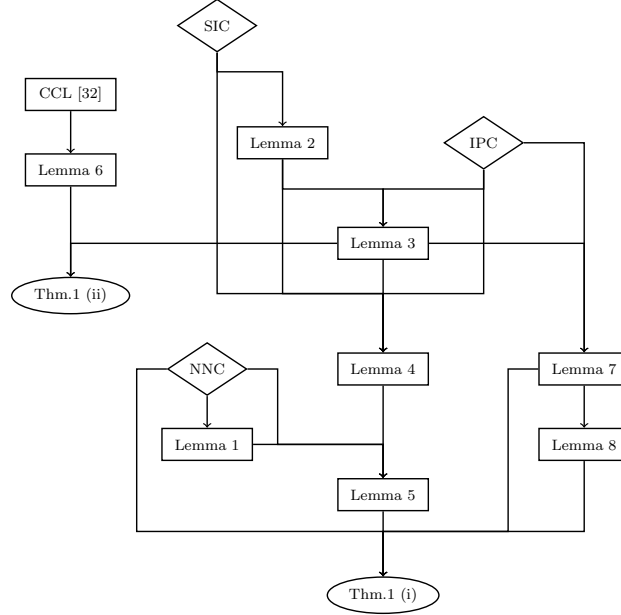


Fig. 8: Connections between Assumptions (diamonds), Lemmas (rectangles), and DPB-spline properties (ellipses).

Lemma 2 *Two patch B-splines $\beta^k \in B^k$ and $\beta^\ell \in B^\ell$ with intersecting supports,*

$$\emptyset \neq \text{supp}\beta^k \cap \text{supp}\beta^\ell \subseteq \Gamma_{\mathcal{D}}^\ell, \text{ with } \ell < k \in \mathcal{D},$$

satisfy

$$\text{supp}\beta^k \cap \Gamma_{\mathcal{D}}^\ell \subseteq \text{supp}\beta^\ell \cap \Gamma_{\mathcal{D}}^\ell, \quad (10)$$

if $\lambda_{\beta^k}(\hat{\beta}^\ell) \neq 0$.

Proof The existence of non-zero coefficients $\lambda_{\beta^k}(\hat{\beta}^\ell) \neq 0$ implies $\text{supp}\beta^k \subseteq \text{supp}\hat{\beta}^\ell$, hence

$$\text{supp}\beta^k \cap \Gamma_{\mathcal{D}}^\ell \subseteq \text{supp}\hat{\beta}^\ell \cap \Gamma_{\mathcal{D}}^\ell. \quad (11)$$

We distinguish between several cases: First, we assume that $\text{supp}\hat{\beta}^\ell \cap \pi^\ell$ is connected. This leads immediately to (10) since $\beta^\ell = \hat{\beta}^\ell|_{\pi^\ell}$ and $\Gamma_{\mathcal{D}}^\ell \subseteq \pi^\ell$.

Second, we consider the case that $\text{supp}\hat{\beta}^\ell \cap \pi^\ell$ possesses two connected components. Thus, besides β^ℓ , there exists another patch B-spline β'^ℓ such that $\text{supp}\beta^\ell \cap \text{supp}\beta'^\ell = \emptyset$ and

$$\text{supp}\hat{\beta}^\ell \cap \pi^\ell = \text{supp}\beta^\ell \cup \text{supp}\beta'^\ell. \quad (12)$$

The intersection of $\text{supp}\beta^k \cap \text{supp}\beta^\ell$ belongs to the constraining boundary $\Gamma_{\mathcal{D}}^\ell$, thus

$$\emptyset \neq \text{supp}\beta^k \cap \text{supp}\beta^\ell = \text{supp}\beta^k \cap \text{supp}\beta^\ell \cap \Gamma_{\mathcal{D}}^\ell. \quad (13)$$

According to SIC and Eq. (3), $\text{supp}\beta^k \cap \Gamma_{\mathcal{D}}^\ell$ is connected. Since the two parts $\text{supp}\beta^\ell \cap \Gamma_{\mathcal{D}}^\ell$ and $\text{supp}\beta^{\ell'} \cap \Gamma_{\mathcal{D}}^\ell$ of the constraining boundary are disjoint it follows that

$$\text{supp}\beta^k \cap \text{supp}\beta^{\ell'} \cap \Gamma_{\mathcal{D}}^\ell = \emptyset. \quad (14)$$

We observe that (11) is equivalent to

$$(\text{supp}\beta^k \cap \Gamma_{\mathcal{D}}^\ell) \cap (\text{supp}\hat{\beta}^\ell \cap \Gamma_{\mathcal{D}}^\ell) = \text{supp}\beta^k \cap \Gamma_{\mathcal{D}}^\ell. \quad (15)$$

We use (12) $\Gamma_{\mathcal{D}}^\ell \subseteq \pi^\ell$ to rewrite the left-hand side of this equation as

$$\text{supp}\beta^k \cap \text{supp}\hat{\beta}^\ell \cap \Gamma_{\mathcal{D}}^\ell = \text{supp}\beta^k \cap (\text{supp}\beta^\ell \cup \text{supp}\beta^{\ell'}) \cap \Gamma_{\mathcal{D}}^\ell.$$

We simplify the result with the help of (13) and (14),

$$\text{supp}\beta^k \cap (\text{supp}\beta^\ell \cup \text{supp}\beta^{\ell'}) \cap \Gamma_{\mathcal{D}}^\ell = \text{supp}\beta^k \cap \text{supp}\beta^\ell \cap \Gamma_{\mathcal{D}}^\ell.$$

Therefore, (15) is equivalent to

$$(\text{supp}\beta^k \cap \Gamma_{\mathcal{D}}^\ell) \cap (\text{supp}\beta^\ell \cap \Gamma_{\mathcal{D}}^\ell) = \text{supp}\beta^k \cap \Gamma_{\mathcal{D}}^\ell.$$

This confirms that

$$\text{supp}\beta^k \cap \Gamma_{\mathcal{D}}^\ell \subseteq \text{supp}\beta^\ell \cap \Gamma_{\mathcal{D}}^\ell.$$

Finally we note that the proof in case two can be extended to more than two connected components. \square

The next Lemma characterizes the intersection of a truncated patch B-spline $\tilde{\beta}_{\mathcal{D}}^k$, for $k \in \mathcal{D}$, with a lower level constraining boundary $\Gamma_{\mathcal{D}}^\ell$, see Fig. 9.

Lemma 3 *The truncated patch B-splines $\tilde{\beta}_{\mathcal{D}}^k \in T^k$ satisfy*

$$\text{supp}\tilde{\beta}_{\mathcal{D}}^k \cap \Gamma_{\mathcal{D}}^\ell \neq \emptyset \Leftrightarrow \text{supp}\beta^k \cap \Gamma_{\mathcal{D}}^\ell \neq \emptyset$$

if $k > \ell$ and $k \in \mathcal{D}$.

Proof According to the definition of the truncated functions, $\text{supp}\beta^k \cap \Gamma_{\mathcal{D}}^\ell \neq \emptyset$ implies that $\text{supp}\tilde{\beta}_{\mathcal{D}}^k \cap \Gamma_{\mathcal{D}}^\ell \neq \emptyset$. In order to prove the other implication, we assume that there exists a $\tilde{\beta}_{\mathcal{D}}^k \in T^k$ such that

$$\text{supp}\tilde{\beta}_{\mathcal{D}}^k \cap \Gamma_{\mathcal{D}}^\ell \neq \emptyset, \quad \text{for } \ell < k,$$

but

$$\text{supp}\beta^k \cap \Gamma_{\mathcal{D}}^\ell = \emptyset. \quad (16)$$

It follows that

$$\text{supp}\tilde{\beta}_{\mathcal{D}}^k \cap (\Delta_{\mathcal{D}, \geq k+1} \setminus \pi^k) \cap \Gamma_{\mathcal{D}}^\ell \neq \emptyset,$$

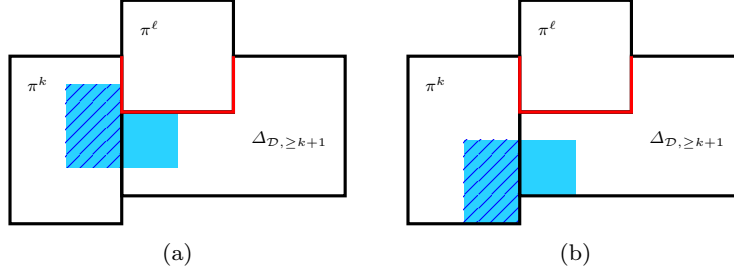


Fig. 9: According to Lemma 3, the supports $\text{supp}\beta^k$ (hatched blue) and $\text{supp}\tilde{\beta}_D^k$ (hatched blue and blue) either intersect both with Γ_D^ℓ (red) or not, see (a) and (b), respectively.

since $\tilde{\beta}_D^k$ takes non-zero values only on the associated patch and on the subdomain $\Delta_{D, \geq k+1}$. Among all such functions we pick one where k is maximal. The representation

$$\tilde{\beta}_D^k = \sum_{\substack{\tilde{\beta}_D^m \in P_D^{k+1} \\ \text{supp}\beta^m \cap \text{supp}\beta^k \neq \emptyset}} \lambda_{\beta^m}(\hat{\beta}^k) \tilde{\beta}_D^m \quad \text{on } \Delta_{D, \geq k+1},$$

see (6), implies that there exists a function $\tilde{\beta}_D^m \in P_D^{k+1}$ with $\text{supp}\beta^m \cap \text{supp}\beta^k \neq \emptyset$ such that

$$\text{supp}\tilde{\beta}_D^m \cap \Gamma_D^\ell \neq \emptyset.$$

It follows immediately that

$$\text{supp}\beta^m \cap \Gamma_D^\ell \neq \emptyset,$$

since k is the largest level with the property (16). Furthermore, $\text{supp}\beta^m \cap \text{supp}\beta^k \neq \emptyset$ implies that $\text{supp}\beta^m \cap \Gamma_D^k \neq \emptyset$, and hence

$$\emptyset \neq \text{supp}\beta^m \cap \Gamma_D^k \cap \Gamma_D^\ell \subseteq \text{supp}\beta^k \cap \Gamma_D^k \cap \Gamma_D^\ell = \emptyset,$$

where the first equation holds according to IPC, the second statement follows from Lemma 2, and the last equality is obtained by (16). This is a contradiction. \square

Lemma 3 enables us to reformulate the selection mechanism. More precisely, instead of considering the truncated patch B-spline $\tilde{\beta}_D^k$ it suffices to analyze whether the associated patch B-spline β^k vanishes on the constraining boundary,

$$S_D^{\ell+1} = \{\tilde{\beta}_D^k \in P_D^{\ell+1} : \beta^k = 0 \quad \text{on } \Gamma_D^\ell\}.$$

Next, we observe that the truncated patch B-splines $\tilde{\beta}_{\mathcal{D}}^k \in T^k$ inherit the support intersection property:

Lemma 4 *The intersections of the supports of truncated patch B-splines $\tilde{\beta}_{\mathcal{D}}^k \in T^k$ with constraining boundaries*

$$\text{supp}\tilde{\beta}_{\mathcal{D}}^k \cap \Gamma_{\mathcal{D}}^\ell \text{ where } \ell < k \quad (17)$$

are connected.

Proof Assume there exists a truncated patch B-spline $\tilde{\beta}_{\mathcal{D}}^k$ whose support intersects the lower level constraining boundary $\Gamma_{\mathcal{D}}^\ell$ in more than one connected component. Among all those functions we choose one where $k \in \mathcal{D}$ is maximal. The intersection splits into two disjoint sets $\delta_1 \neq \emptyset$ and $\delta_2 \neq \emptyset$ with $\delta_1 \cap \delta_2 = \emptyset$ such that

$$\text{supp}\tilde{\beta}_{\mathcal{D}}^k \cap \Gamma_{\mathcal{D}}^\ell = \delta_1 \cup \delta_2. \quad (18)$$

SIC requires that $\text{supp}\beta^k \cap \Gamma_{\mathcal{D}}^\ell$ is connected. Since $\text{supp}\beta^k \subseteq \text{supp}\tilde{\beta}_{\mathcal{D}}^k$, this implies that $\text{supp}\beta^k \cap \Gamma_{\mathcal{D}}^\ell$ is a subset of one δ_i whereas its intersection with the other one is empty. Without loss of generality we assume

$$\text{supp}\beta^k \cap \Gamma_{\mathcal{D}}^\ell \subseteq \delta_1 \quad \text{and} \quad \text{supp}\beta^k \cap \delta_2 = \emptyset. \quad (19)$$

According to the latter observation, the truncated patch B-spline $\tilde{\beta}_{\mathcal{D}}^k$ intersects δ_2 in patches of levels higher than k , i.e.,

$$\text{supp}\tilde{\beta}_{\mathcal{D}}^k \cap (\Delta_{\mathcal{D}, \geq k+1} \setminus \pi^k) \cap \delta_2 \neq \emptyset.$$

Due to the definition of the truncation (6), there exists a function $\tilde{\beta}_{\mathcal{D}}^m \in P_{\mathcal{D}}^{k+1}$ with $\text{supp}\beta^m \cap \text{supp}\beta^k \neq \emptyset$ that satisfies

$$\text{supp}\tilde{\beta}_{\mathcal{D}}^m \cap \delta_2 \neq \emptyset. \quad (20)$$

Moreover, we have

$$\text{supp}\tilde{\beta}_{\mathcal{D}}^m \cap \Gamma_{\mathcal{D}}^\ell \subseteq \text{supp}\tilde{\beta}_{\mathcal{D}}^k \cap \Gamma_{\mathcal{D}}^\ell = \delta_1 \cup \delta_2.$$

Recall that we assumed k to be maximal. Thus $\text{supp}\tilde{\beta}_{\mathcal{D}}^m \cap \Gamma_{\mathcal{D}}^\ell$ is connected and we obtain

$$\text{supp}\tilde{\beta}_{\mathcal{D}}^m \cap \delta_1 = \emptyset. \quad (21)$$

From $\text{supp}\beta^m \cap \text{supp}\beta^k \neq \emptyset$ it follows that $\text{supp}\beta^m \cap \Gamma_{\mathcal{D}}^k \neq \emptyset$. Furthermore, (20) leads to

$$\emptyset \neq \text{supp}\tilde{\beta}_{\mathcal{D}}^m \cap \delta_2 \subseteq \text{supp}\tilde{\beta}_{\mathcal{D}}^m \cap \Gamma_{\mathcal{D}}^\ell,$$

since (18) implies that $\delta_2 \subseteq \Gamma_{\mathcal{D}}^\ell$. According to Lemma 3 $\text{supp}\tilde{\beta}_{\mathcal{D}}^m \cap \Gamma_{\mathcal{D}}^\ell \neq \emptyset$ is equivalent to $\text{supp}\beta^m \cap \Gamma_{\mathcal{D}}^\ell \neq \emptyset$. Applying IPC leads to

$$\text{supp}\beta^m \cap \Gamma_{\mathcal{D}}^k \cap \Gamma_{\mathcal{D}}^\ell \neq \emptyset.$$

Furthermore, Lemma 2 states that $\text{supp}\beta^m \cap \Gamma_{\mathcal{D}}^k \subseteq \text{supp}\beta^k \cap \Gamma_{\mathcal{D}}^k$. Combining these observations with simple subset relations and (19) results in the following equations,

$$\emptyset \neq \text{supp}\beta^m \cap \Gamma_{\mathcal{D}}^k \cap \Gamma_{\mathcal{D}}^\ell \subseteq \text{supp}\beta^k \cap \Gamma_{\mathcal{D}}^k \cap \Gamma_{\mathcal{D}}^\ell \subseteq \text{supp}\beta^k \cap \Gamma_{\mathcal{D}}^\ell \subseteq \delta_1.$$

However, this implies that

$$\emptyset \neq \text{supp}\beta^m \cap \delta_1 \subseteq \text{supp}\tilde{\beta}_{\mathcal{D}}^m \cap \delta_1,$$

which contradicts (21), and thereby completes the proof. \square

Finally we present an extension of Lemma 2.

Lemma 5 *The supports of truncated patch B-splines $\tilde{\beta}_{\mathcal{D}}^k \in P_{\mathcal{D}}^{\ell+1}$ and patch B-splines $\beta^\ell \in B^\ell$ of lower level $\ell < k$ satisfy*

$$\text{supp}\tilde{\beta}_{\mathcal{D}}^k \cap \Gamma_{\mathcal{D}}^\ell \subseteq \text{supp}\beta^\ell \cap \Gamma_{\mathcal{D}}^\ell,$$

if $\text{supp}\beta^k \cap \text{supp}\beta^\ell \neq \emptyset$ and $\lambda_{\beta^k}(\hat{\beta}^\ell) \neq 0$.

Proof The proof works similar to the proof of Lemma 2. We do not provide all details but show how to adapt it to the current situation.

Recall that $\lambda_{\beta^k}(\hat{\beta}^\ell) \neq 0$ implies $\text{supp}\hat{\beta}^k \subseteq \text{supp}\hat{\beta}^\ell$. From Lemma 1 it follows that $\text{supp}\tilde{\beta}_{\mathcal{D}}^k \subseteq \text{supp}\hat{\beta}^\ell$ and thus,

$$\text{supp}\tilde{\beta}_{\mathcal{D}}^k \cap \Gamma_{\mathcal{D}}^\ell \subseteq \text{supp}\hat{\beta}^\ell \cap \Gamma_{\mathcal{D}}^\ell.$$

As in Lemma 2, the proof follows immediately for the case that $\text{supp}\hat{\beta}^\ell \cap \pi^\ell$ possesses one connected component. For the other case we note that

$$\emptyset \neq \text{supp}\beta^k \cap \text{supp}\beta^\ell \cap \Gamma_{\mathcal{D}}^\ell \subseteq \text{supp}\tilde{\beta}_{\mathcal{D}}^k \cap \text{supp}\beta^\ell \cap \Gamma_{\mathcal{D}}^\ell,$$

according to the assumption that $\text{supp}\beta^k \cap \text{supp}\beta^\ell \neq \emptyset$. Using Lemma 4 allows us to proceed as in the proof of Lemma 2 using $\tilde{\beta}_{\mathcal{D}}^k$ instead of β^k . \square

We introduce the notion of *homogeneous boundary conditions*: A C^s -smooth function f satisfies homogeneous boundary conditions in a point \mathbf{x} if the values of the function and of all its partial derivatives up to order $s_k = p_k - 1$ in all variables separately³ are equal to zero,

$$\vartheta f(\mathbf{x}) = 0,$$

with

³ For instance, $f = f_x = f_y = f_{xx} = f_{xy} = f_{yy} = f_{xxy} = f_{xyy} = f_{xxyy} = 0$ for $\mathbf{x} = (x, y)$ and $\mathbf{s} = (2, 2)$.

$$[\partial f(\mathbf{x})]_{\mathbf{i}} = \partial_{\mathbf{i}} f(\mathbf{x}), \quad \mathbf{i} = (i_1, \dots, i_d), \quad i_k \leq p_k - 1.$$

and partial derivative operators

$$(\partial_{\mathbf{i}} f)(\mathbf{x}) = \frac{\partial^{i_1}}{\partial x_1^{i_1}} \cdots \frac{\partial^{i_d}}{\partial x_d^{i_d}} f(x_1, \dots, x_d).$$

Since π^ℓ can be divided into a set of cells $z \in Z^\ell$, the boundary of a patch π^ℓ naturally splits into facets ξ of different dimensions. E.g., the facets can be edges or vertices of cells of level ℓ for dimension $d = 2$, see also the Appendix of [10].

Lemma 6 *If a function $f \in \mathbb{V}^\ell$ satisfies homogeneous boundary conditions on a boundary facet ξ of π^ℓ , then $\lambda_{\beta^\ell}(f) = 0$ if $\xi \subseteq \text{supp}\beta^\ell$.*

Proof We note that for a cell $z \in Z^\ell$ and every $\beta^\ell \in B^\ell$ that does not vanish on that cell, i.e., $z \subseteq \text{supp}\beta^\ell$, it holds that

$$0 \neq \beta^\ell|_z = \tilde{\beta}^\ell|_z,$$

according to (4). Suitably adapting the proof of Lemma 2 in [10], which is based on the Contact Characterization Lemma (CCL) in [32], confirms this fact. \square

4.2.2 Proof of the theorem

Finally, we can prove the results stated in Theorem 1. We prove the statements (i)-(iv) for all subdomains $\Delta_{\mathcal{D}} \subseteq \Delta_{\geq \ell}$, i.e., $\mathcal{D} \subseteq \{\ell, \dots, N\}$, by induction over ℓ , proceeding from the maximum level N down to 1.

For $\ell = N$ we note that $\Delta_{\geq N} = \pi^N$. Therefore, a subdomain of $\Delta_{\geq N}$ is either the empty set (trivial case) or $\mathcal{D} = \{N\}$. Then $P_{\mathcal{D}} = T_{\mathcal{D}}^N$ consists of functions

$$\tilde{\beta}_{\mathcal{D}}^N = \begin{cases} \beta^N & \text{on } \pi^N \\ 0 & \text{elsewhere} \end{cases}.$$

Therefore, we can conclude that (i)-(iv) are satisfied for any subdomain $\Delta_{\mathcal{D}} \subseteq \Delta_{\geq N}$. Now we assume that (i)-(iv) are satisfied for any subdomain $\Delta_{\mathcal{D}} \subseteq \Delta_{\geq \ell+1}$. We show that the properties extend to any subdomain $\Delta_{\mathcal{D}} \subseteq \Delta_{\geq \ell}$. We consider only the case where $\ell \in \mathcal{D}$, hence $\mathcal{D} \subseteq \{\ell, \dots, N\}$. Otherwise, the result follows immediately from the induction hypothesis.

First statement (i): We have that

$$P_{\mathcal{D}} = P_{\mathcal{D}}^1 = P_{\mathcal{D}}^\ell = T_{\mathcal{D}}^\ell \cup S_{\mathcal{D}}^{\ell+1}.$$

For functions in $S_{\mathcal{D}}^{\ell+1}$ the smoothness on $\Delta_{\mathcal{D}} = \Delta_{\mathcal{D}, \geq \ell}$ follows from the induction hypothesis combined with the fact that the functions are zero on

π^ℓ and satisfy homogeneous boundary conditions on $\Gamma_{\mathcal{D}}^\ell$ according to the selection mechanism. Next we consider a function $\tilde{\beta}_{\mathcal{D}}^\ell \in T_{\mathcal{D}}^\ell$. We note that $\tilde{\beta}_{\mathcal{D}}^\ell$ obviously possesses the required smoothness on π^ℓ and also on $\Delta_{\mathcal{D}, \geq \ell+1} \setminus \pi^\ell$ (considered separately). Indeed, its restriction to the latter domain is a linear combination of functions in $P_{\mathcal{D}}^{\ell+1}$, which satisfy the smoothness conditions according to the induction hypothesis.

Now it remains to be shown that $\tilde{\beta}_{\mathcal{D}}^\ell$ possesses the required order of smoothness on the constraining boundary $\Gamma_{\mathcal{D}}^\ell$. According to NNC it holds that $\hat{\beta}^\ell \in \mathbb{P}_{\mathcal{N}_{\mathcal{D}}^\ell}$. From the induction hypothesis (ii) it follows that there exists a representation,

$$\hat{\beta}^\ell = \sum_{\tilde{\beta}_{\mathcal{N}_{\mathcal{D}}^\ell}^k \in P_{\mathcal{N}_{\mathcal{D}}^\ell}} \lambda_{\beta^k}(\hat{\beta}^\ell) \tilde{\beta}_{\mathcal{N}_{\mathcal{D}}^\ell}^k \quad \text{on } \Delta_{\mathcal{N}_{\mathcal{D}}^\ell}.$$

We use it to define the auxiliary function

$$\hat{\beta}_{\mathcal{N}_{\mathcal{D}}^\ell}^\ell = \sum_{\substack{\tilde{\beta}_{\mathcal{N}_{\mathcal{D}}^\ell}^k \in P_{\mathcal{N}_{\mathcal{D}}^\ell} \\ \text{supp}\beta^k \cap \text{supp}\beta^\ell \neq \emptyset}} \lambda_{\beta^k}(\hat{\beta}^\ell) \tilde{\beta}_{\mathcal{N}_{\mathcal{D}}^\ell}^k, \quad (22)$$

by considering only functions near the boundary to $\text{supp}\beta^\ell$ and observe that

$$\vartheta \hat{\beta}_{\mathcal{N}_{\mathcal{D}}^\ell}^\ell = \vartheta \hat{\beta}^\ell = \vartheta \beta^\ell \quad \text{on } \Gamma_{\mathcal{D}}^\ell \cap \text{supp}\beta^\ell.$$

Furthermore, it holds that

$$\vartheta \hat{\beta}_{\mathcal{N}_{\mathcal{D}}^\ell}^\ell = \vartheta \beta^\ell = 0 \quad \text{on } \Gamma_{\mathcal{D}}^\ell \setminus \text{supp}\beta^\ell,$$

since $\text{supp}\tilde{\beta}_{\mathcal{N}_{\mathcal{D}}^\ell}^k \cap \Gamma_{\mathcal{N}_{\mathcal{D}}^\ell}^\ell \subseteq \text{supp}\beta^\ell \cap \Gamma_{\mathcal{N}_{\mathcal{D}}^\ell}^\ell$ according to Lemma 5 and $\Gamma_{\mathcal{N}_{\mathcal{D}}^\ell}^\ell = \Gamma_{\mathcal{D}}^\ell$.

Therefore, we obtain that $\vartheta \hat{\beta}_{\mathcal{N}_{\mathcal{D}}^\ell}^\ell = \vartheta \beta^\ell$ on $\Gamma_{\mathcal{D}}^\ell$.

Now we show that the auxiliary function shares values and derivatives with the truncated function along the constraining boundary, $\vartheta \hat{\beta}_{\mathcal{N}_{\mathcal{D}}^\ell}^\ell = \vartheta \tilde{\beta}_{\mathcal{D}}^\ell$ on $\Gamma_{\mathcal{D}}^\ell$. More precisely, we prove that

$$\vartheta \left(\sum_{\substack{\tilde{\beta}_{\mathcal{N}_{\mathcal{D}}^\ell}^k \in P_{\mathcal{N}_{\mathcal{D}}^\ell} \\ \text{supp}\beta^k \cap \text{supp}\beta^\ell \neq \emptyset}} \lambda_{\beta^k}(\hat{\beta}^\ell) \tilde{\beta}_{\mathcal{N}_{\mathcal{D}}^\ell}^k \right) = \vartheta \left(\sum_{\substack{\tilde{\beta}_{\mathcal{D}}^k \in P_{\mathcal{D}}^{\ell+1} \\ \text{supp}\beta^k \cap \text{supp}\beta^\ell \neq \emptyset}} \lambda_{\beta^k}(\hat{\beta}^\ell) \tilde{\beta}_{\mathcal{D}}^k \right), \quad \text{on } \Gamma_{\mathcal{D}}^\ell. \quad (23)$$

We note that

$$\text{supp}\beta^k \cap \text{supp}\beta^\ell \neq \emptyset \Rightarrow \beta^k|_{\Gamma_{\mathcal{D}}^\ell} \neq 0, \quad \text{if } k > \ell.$$

The proof of (23) is based on two technical Lemmas. The first one states that the selection mechanism always selects the same functions for \mathcal{D} and $\mathcal{N}_{\mathcal{D}}^\ell$.

Lemma 7 For all $\beta^k \in B^k$ with $\beta^k \neq 0$ on $\Gamma_{\mathcal{D}}^\ell$ it holds that

$$\tilde{\beta}_{\mathcal{N}_{\mathcal{D}}^\ell}^k \in P_{\mathcal{N}_{\mathcal{D}}^\ell}^m \Leftrightarrow \tilde{\beta}_{\mathcal{D}}^k \in P_{\mathcal{D}}^m, \quad (24)$$

if $k \geq m > \ell$.

Proof On the one hand, we consider a function $\tilde{\beta}_{\mathcal{D}}^k \in P_{\mathcal{D}}^m$ with $\text{supp}\beta^k \cap \Gamma_{\mathcal{D}}^\ell \neq \emptyset$. Hence, $k \in \mathcal{N}_{\mathcal{D}}^\ell$. We note that

$$P_{\mathcal{D}}^m = \bigcup_{k \in \mathcal{D}, k \geq m} \{\tilde{\beta}_{\mathcal{D}}^k \in T_{\mathcal{D}}^k : \text{supp}\beta^k \cap \Gamma_{\mathcal{D}}^r = \emptyset, \text{ for all } r \in \mathcal{D}, m \leq r < k\} \quad (25)$$

and

$$P_{\mathcal{N}_{\mathcal{D}}^\ell}^m = \bigcup_{k \in \mathcal{N}_{\mathcal{D}}^\ell, k \geq m} \{\tilde{\beta}_{\mathcal{N}_{\mathcal{D}}^\ell}^k \in T_{\mathcal{N}_{\mathcal{D}}^\ell}^k : \text{supp}\beta^k \cap \Gamma_{\mathcal{N}_{\mathcal{D}}^\ell}^r = \emptyset \text{ for all } r \in \mathcal{N}_{\mathcal{D}}^\ell, m \leq r < k\},$$

according to the selection mechanism and Lemma 3. Since $\Gamma_{\mathcal{N}_{\mathcal{D}}^\ell}^r \subseteq \Gamma_{\mathcal{D}}^r$ for $r \in \mathcal{N}_{\mathcal{D}}^\ell$, the first condition $\text{supp}\beta^k \cap \Gamma_{\mathcal{D}}^r = \emptyset$ implies $\text{supp}\beta^k \cap \Gamma_{\mathcal{N}_{\mathcal{D}}^\ell}^r = \emptyset$ if $m \leq r < k$. Therefore, we conclude that $\tilde{\beta}_{\mathcal{N}_{\mathcal{D}}^\ell}^k \in P_{\mathcal{N}_{\mathcal{D}}^\ell}^m$.

On the other hand, assume there exists a function $\tilde{\beta}_{\mathcal{N}_{\mathcal{D}}^\ell}^k \in P_{\mathcal{N}_{\mathcal{D}}^\ell}^m$ with $\tilde{\beta}_{\mathcal{D}}^k \notin P_{\mathcal{D}}^m$ and $\beta^k \neq 0$ on $\Gamma_{\mathcal{D}}^\ell$. We invoke the characterization (25) to conclude that there exists a level $r \in \mathcal{D} \setminus \mathcal{N}_{\mathcal{D}}^\ell$ and $m \leq r < k$ such that $\text{supp}\beta^k \cap \Gamma_{\mathcal{D}}^r \neq \emptyset$. The considered function satisfies $\text{supp}\beta^k \cap \Gamma_{\mathcal{D}}^\ell \neq \emptyset$ and hence it follows that $\text{supp}\beta^k \cap \Gamma_{\mathcal{D}}^\ell \cap \Gamma_{\mathcal{D}}^r \neq \emptyset$ by IPC. However, since π^r is not a neighbor of π^ℓ it holds that $\Gamma_{\mathcal{D}}^r \cap \Gamma_{\mathcal{D}}^\ell \subseteq \pi^r \cap \pi^\ell = \emptyset$ which implies that $\text{supp}\beta^k \cap \Gamma_{\mathcal{D}}^\ell \cap \Gamma_{\mathcal{D}}^r = \emptyset$. This is a contradiction. \square

The second lemma confirms that the functions considered in the previous lemma possess the same values and derivatives along the constraining boundary.

Lemma 8 For all functions in (24) with $\tilde{\beta}_{\mathcal{D}}^k \in P_{\mathcal{D}}^m$ it holds that

$$\vartheta \tilde{\beta}_{\mathcal{D}}^k = \vartheta \tilde{\beta}_{\mathcal{N}_{\mathcal{D}}^\ell}^k \quad \text{on } \Gamma_{\mathcal{D}}^\ell \cap \Delta_{\mathcal{D}, \geq m}, \quad (26)$$

if $k \geq m > \ell$.

Proof We use induction over the level m from n down to $\ell + 1$ with $n = \max\{k \in \mathcal{N}_{\mathcal{D}}^\ell\}$. It suffices to consider these functions since levels higher than n are not active on $\Gamma_{\mathcal{D}}^\ell$.

For level n it holds that

$$\tilde{\beta}_{\mathcal{D}}^n = \beta^n = \tilde{\beta}_{\mathcal{N}_{\mathcal{D}}^\ell}^n, \quad \text{on } \pi^n,$$

for all $\tilde{\beta}_{\mathcal{D}}^n \in P_{\mathcal{D}}^n$. Thus, $\vartheta \tilde{\beta}_{\mathcal{D}}^n = \vartheta \tilde{\beta}_{N_{\mathcal{D}}^{\ell}}^n$ on $\Gamma_{\mathcal{D}}^{\ell} \cap \Delta_{\mathcal{D}, \geq n}$. In order to complete the proof by induction, we assume that (26) is satisfied for $m+1$ and show that this extends to m .

First, we consider functions $\tilde{\beta}_{\mathcal{D}}^k \in P_{\mathcal{D}}^m$ with $k > m$. The induction hypothesis implies that

$$\vartheta \tilde{\beta}_{\mathcal{D}}^k = \vartheta \tilde{\beta}_{N_{\mathcal{D}}^{\ell}}^k, \quad \text{on } \Gamma_{\mathcal{D}}^{\ell} \cap \Delta_{\mathcal{D}, \geq m+1}.$$

Furthermore, the selection ensures that these functions vanish on π^m , hence

$$\vartheta \tilde{\beta}_{\mathcal{D}}^k = \vartheta \tilde{\beta}_{N_{\mathcal{D}}^{\ell}}^k = 0, \quad \text{on } \Gamma_{\mathcal{D}}^{\ell} \cap \pi^m.$$

The equality on $\Gamma_{\mathcal{D}}^{\ell} \cap \Delta_{\mathcal{D}, \geq m}$ now follows from

$$\Gamma_{\mathcal{D}}^{\ell} \cap \Delta_{\mathcal{D}, \geq m} = (\Gamma_{\mathcal{D}}^{\ell} \cap \pi^m) \cup (\Gamma_{\mathcal{D}}^{\ell} \cap \Delta_{\mathcal{D}, \geq m+1}). \quad (27)$$

Second, we consider the remaining functions $\tilde{\beta}_{\mathcal{D}}^m \in T_{\mathcal{D}}^m$. Obviously, it holds that

$$\vartheta \tilde{\beta}_{\mathcal{D}}^m = \vartheta \tilde{\beta}_{N_{\mathcal{D}}^{\ell}}^m = \vartheta \beta^m, \quad \text{on } \Gamma_{\mathcal{D}}^{\ell} \cap \pi^m.$$

Furthermore,

$$\tilde{\beta}_{\mathcal{D}}^m = \sum_{\substack{\tilde{\beta}_{\mathcal{D}}^r \in P_{\mathcal{D}}^{m+1} \\ \text{supp} \beta^r \cap \text{supp} \beta^m \neq \emptyset}} \lambda_{\beta^r}(\hat{\beta}^m) \tilde{\beta}_{\mathcal{D}}^r \quad \text{on } \Delta_{\mathcal{D}, \geq m+1}.$$

The previous lemma (see (24)) and the induction hypothesis imply

$$\vartheta \left(\sum_{\substack{\tilde{\beta}_{\mathcal{D}}^r \in P_{\mathcal{D}}^{m+1} \\ \text{supp} \beta^r \cap \text{supp} \beta^m \neq \emptyset}} \lambda_{\beta^r}(\hat{\beta}^m) \tilde{\beta}_{\mathcal{D}}^r \right) = \vartheta \left(\sum_{\substack{\tilde{\beta}_{N_{\mathcal{D}}^{\ell}}^r \in P_{N_{\mathcal{D}}^{\ell}}^{m+1} \\ \text{supp} \beta^r \cap \text{supp} \beta^m \neq \emptyset}} \lambda_{\beta^r}(\hat{\beta}^m) \tilde{\beta}_{N_{\mathcal{D}}^{\ell}}^r \right) = \vartheta \tilde{\beta}_{N_{\mathcal{D}}^{\ell}}^m$$

on $\Gamma_{\mathcal{D}}^{\ell} \cap \Delta_{\mathcal{D}, \geq m+1}$. Invoking the decomposition (27) confirms that (26) is satisfied for all $\tilde{\beta}_{\mathcal{D}}^m \in T_{\mathcal{D}}^m$. \square

Now we are able to prove the original statement (23). Applying both Lemmas with $m = \ell + 1$ confirms that $\vartheta \hat{\beta}_{N_{\mathcal{D}}^{\ell}}^{\ell} = \vartheta \beta^{\ell} = \vartheta \tilde{\beta}_{\mathcal{D}}^{\ell}$ on $\Gamma_{\mathcal{D}}^{\ell} = \Gamma_{\mathcal{D}}^{\ell} \cap \Delta_{\mathcal{D}, \geq \ell}$ since $P_{N_{\mathcal{D}}^{\ell}} = P_{N_{\mathcal{D}}^{\ell}}^1 = P_{N_{\mathcal{D}}^{\ell}}^{\ell+1}$. Hence, we conclude that the functions $\tilde{\beta}_{\mathcal{D}}^{\ell} \in T_{\mathcal{D}}^{\ell}$ possess the required order of smoothness on $\Delta_{\mathcal{D}, \geq \ell}$.

Second statement (ii): We consider a function $f \in \mathbb{P}_{\mathcal{D}}$. Its restriction to π^{ℓ} has a representation

$$f = \sum_{\beta^{\ell} \in B^{\ell}} \lambda_{\beta^{\ell}}(f) \beta^{\ell} = \sum_{\beta^{\ell} \in B^{\ell}} \lambda_{\beta^{\ell}}(f) \tilde{\beta}_{\mathcal{D}}^{\ell} \quad \text{on } \pi^{\ell}, \quad (28)$$

since $\beta^{\ell} = \tilde{\beta}_{\mathcal{D}}^{\ell}$ on π^{ℓ} . We now define

$$\tilde{f} = f - \sum_{\beta^\ell \in B^\ell} \lambda_{\beta^\ell}(f) \tilde{\beta}_D^\ell \quad \text{on } \Delta_D. \quad (29)$$

Clearly, \tilde{f} is equal to zero on π^ℓ and satisfies homogeneous boundary conditions on Γ_D^ℓ . We observe that $\tilde{f} \in \mathbb{P}_D^{\ell+1}$. Indeed, the definition of the patchwork spline space \mathbb{P}_D gives $f \in \mathbb{P}_D^{\ell+1}$, and the functions $\tilde{\beta}_D^\ell \in T_D^\ell$ are linear combinations of functions in $\mathbb{P}_D^{\ell+1}$. According to the induction hypothesis there exists a representation

$$\tilde{f} = \sum_{\tilde{\beta}_D^k \in P_D^{\ell+1}} \lambda_{\beta^k}(\tilde{f}) \tilde{\beta}_D^k \quad \text{on } \Delta_{D, \geq \ell+1}. \quad (30)$$

We consider a function $\tilde{\beta}_D^k \in P_D^{\ell+1} \setminus S_D^{\ell+1}$ in the above sum. The definition of $S_D^{\ell+1}$ and Lemma 3 imply that

$$\text{supp} \beta^k \cap \Gamma_D^\ell \neq \emptyset.$$

There exists a facet ξ of $\pi^k \cap \pi^\ell \subseteq \Gamma_D^\ell$ with $\xi \subseteq \text{supp} \beta^k$ where \tilde{f} satisfies the homogeneous boundary conditions. Therefore, we can apply Lemma 6 and obtain that $\lambda_{\beta^k}(\tilde{f}) = 0$.

Consequently, only functions in $S_D^{\ell+1}$ contribute to the representation in (30) and thus, we can extend this representation to Δ_D ,

$$\tilde{f} = \sum_{\tilde{\beta}_D^k \in S_D^{\ell+1}} \lambda_{\beta^k}(\tilde{f}) \tilde{\beta}_D^k \quad \text{on } \Delta_D. \quad (31)$$

Therefore, we can combine equations (29) and (31) to represent f with respect to P_D on Δ_D ,

$$f = \sum_{\tilde{\beta}^k \in P_D} \mu_{\tilde{\beta}^k}(f) \tilde{\beta}_D^k \quad \text{on } \Delta_D, \quad (32)$$

with coefficients

$$\mu_{\tilde{\beta}_D^k}(f) = \begin{cases} \lambda_{\beta^\ell}(f) & \text{if } k = \ell \\ \lambda_{\beta^k}(\tilde{f}) & \text{otherwise.} \end{cases}$$

Finally, we note that the functions in P_D are linearly independent. Indeed, T_D^ℓ is linearly independent on π^ℓ , since $\tilde{\beta}_D^\ell = \beta^\ell$ on π^ℓ and the functions β^ℓ are linearly independent on π^ℓ . Moreover, the remaining functions in $S_D^{\ell+1} \subseteq P_D^{\ell+1}$ vanish on π^ℓ while being linearly independent on $\Delta_{D, \geq \ell+1}$ according to the induction hypothesis.

Third statement (iii): We rewrite Equation (32) by using the definition of the DPB-splines P_D and obtain

$$f = \sum_{\tilde{\beta}_D^\ell \in T_D^\ell} \mu_{\tilde{\beta}_D^\ell}(f) \tilde{\beta}_D^\ell + \sum_{\tilde{\beta}_D^k \in S_D^{\ell+1}} \mu_{\tilde{\beta}_D^k}(f) \tilde{\beta}_D^k \quad \text{on } \Delta_D. \quad (33)$$

This confirms (9) with respect to the patch B-splines on π^ℓ since $\mu_{\tilde{\beta}_D^\ell}(f) = \lambda_{\beta^\ell}(f)$.

Next we consider the restriction of f to $\Delta_{D, \geq \ell+1}$. On the one hand, it satisfies

$$f = \sum_{\tilde{\beta}_D^k \in P_D^{\ell+1}} \lambda_{\beta^k}(f) \tilde{\beta}_D^k \quad \text{on } \Delta_{D, \geq \ell+1}, \quad (34)$$

according to the induction hypothesis (ii). On the other hand, we may rewrite (33) as

$$f = \underbrace{\sum_{\tilde{\beta}_D^\ell \in T_D^\ell} \lambda_{\beta^\ell}(f) \sum_{\substack{\tilde{\beta}_D^k \in P_D^{\ell+1} \\ \text{supp } \beta^\ell \cap \text{supp } \beta^k \neq \emptyset}} \lambda_{\beta^k}(\hat{\beta}^\ell) \tilde{\beta}_D^k}_{(\star)} + \sum_{\tilde{\beta}_D^k \in S_D^{\ell+1}} \mu_{\tilde{\beta}_D^k}(f) \tilde{\beta}_D^k$$

on $\Delta_{D, \geq \ell+1}$, according to the definition of the truncation operator. Note that none of the functions $\tilde{\beta}_D^k$ that appear in the double sum (\star) belong to the set $S_D^{\ell+1}$ of selected functions, since $\text{supp } \beta^\ell \cap \text{supp } \beta^k \neq \emptyset$ implies that $\beta^k \neq 0$ on Γ_D^ℓ . Therefore, comparing the coefficients with (34) confirms that $\mu_{\tilde{\beta}_D^k}(f) = \lambda_{\beta^k}(f)$ for $\tilde{\beta}_D^k \in S_D^{\ell+1}$.

Fourth statement (iv): First, we show that the basis functions in $P_D^\ell = T_D^\ell \cup S_D^{\ell+1}$ are non-negative on Δ_D .

Since $S_D^{\ell+1} \subseteq P_D^{\ell+1}$ the induction hypothesis implies that functions in $S_D^{\ell+1}$ are non-negative on $\Delta_{D, \geq \ell+1}$. This extends to Δ_D as these functions vanish on π^ℓ according to the selection mechanism. The functions in T_D^ℓ are non-negative on π^ℓ since there $\tilde{\beta}_D^\ell = \beta^\ell$ and the functions β^ℓ are non-negative. Moreover, their representation with respect to $P_D^{\ell+1} \setminus S_D^{\ell+1}$ on $\Delta_{D, \geq \ell+1}$ is a linear combination of non-negative functions with non-negative coefficients.

Second, we note that the partition of unity is obtained by applying (9) to the function $f = 1$.

This completes the proof of Theorem 1.

5 Comparison with THB- and TPB-splines

This section is used for comparing the flexibility of DPB-, TPB- and THB-splines. First, we observe that the new construction of DPB-splines complements the other two bases. To be more precise, on some hierarchies we can construct only one of the bases while on others we can define two or even all three of them.

Example 4 We consider several instances of hierarchical meshes for spline spaces of degree $\mathbf{p} = (2, 2)$ and discuss if the hierarchies possess a DPB-

spline basis, see Fig. 10. Note that IPC and SIC are automatically satisfied for a patch π^ℓ if it shares its boundary with higher level patches only, e.g., as it is the case for the first patch π^1 . Furthermore, if a patch of level ℓ shares its boundary with only one patch of lower level $k < \ell$ then IPC and SIC are satisfied for π^ℓ . Moreover, we analyze if we can construct a TPB-spline basis or a THB-spline basis on these meshes:

- A hierarchy is feasible for THB-splines if the spline spaces of all levels are nested [18].
- For TPB-splines the FSC (“full shadow compatibility”) and CBA (“constrained boundary alignment”) assumption, see [10], have to be fulfilled in order to obtain a basis. Note that CBA is satisfied if all patches are aligned with the knot lines of the corresponding spline space.

We observe that the new construction of DPB-splines complements the other two bases.

Although there exist hierarchies that are valid for TPB- and not for DPB-splines we conjecture that this set is rather small compared to the set of hierarchies that possess a DPB- and no TPB-spline basis. The following example supports this assumption.

Example 5 We consider the regular subdivision of the unit square into 4×4 patches and randomly assign values from 0 to 3 to each patch. The spline spaces of the patches remain unchanged, are refined dyadically in x_1 -direction, in x_2 -direction and in both directions for the values 0, 1, 2 and 3, respectively. The patches are sorted according to these values, and patches with the same value are ordered randomly. We compute 120,000 samples of such random hierarchies and analyze how many of them are feasible for TPB- and DPB-splines. The results are reported in Table 1. Most of the samples (114,605) do not satisfy NNC and are unsuitable for all constructions. From the remaining 5,395 hierarchies, 588 (approx. 11%) can be equipped with a DPB-spline basis, but only 4 (approx. 0.07%) admit a TPB-spline basis. 3 hierarchies are valid for TPB- and DPB-splines. The same experiment was performed for bicubic splines, on 3×3 patches with triadic refinement, see Table 1 last row. Finally, we note that very few (2 and 231) of the 120,000 samples did not use anisotropic refinement, i.e., not the refinement values 1 and 2.

	nested	DPB	TPB	both
$\mathbf{p} = (2, 2)$, 4×4 patches	5,395	588	4	3
$\mathbf{p} = (3, 3)$, 3×3 patches	25,169	11,636	2,011	1,757

Table 1: Example 5 – Experimental quantification of patch structures suitable for TPB- and DPB-splines.

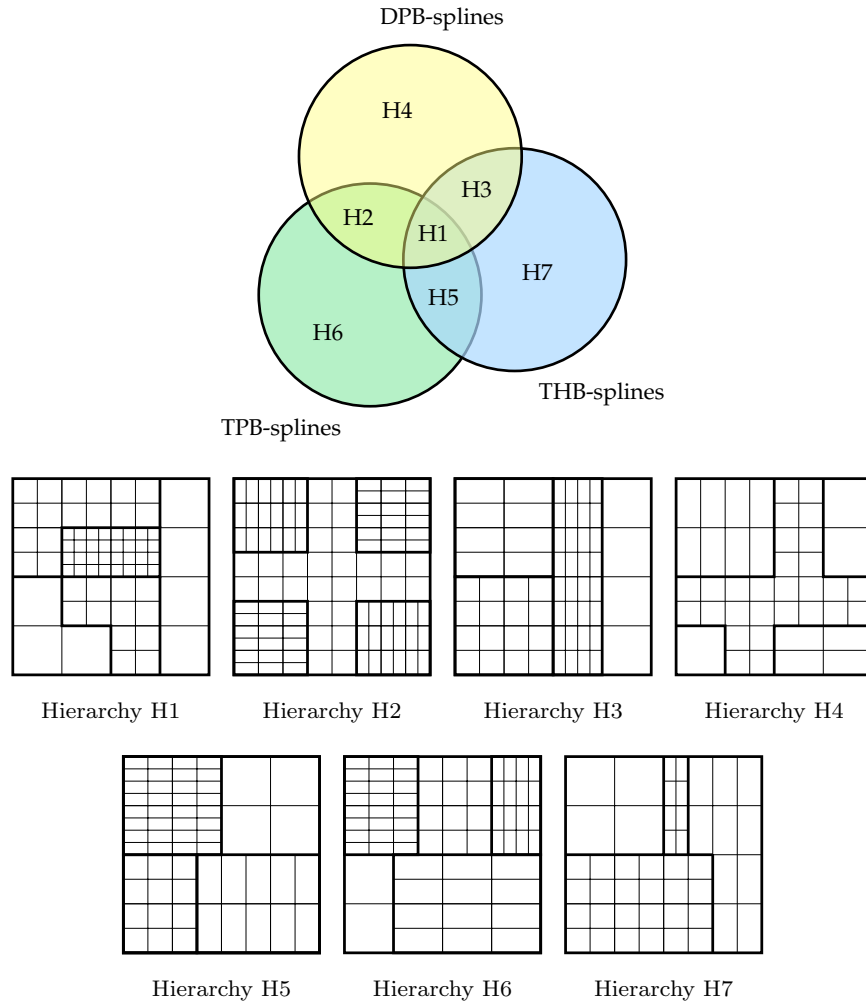


Fig. 10: Venn diagram and hierarchical meshes for DPB-, TPB- and THB-splines.

6 Macro element refinement for adaptive surface reconstruction

We present an adaptive refinement algorithm for surface approximation that generates a two-dimensional patchwork hierarchy where NNC, IPC and SIC are satisfied. Thus, a DPB-spline fitting surface can be constructed on the patch structure. In contrast to our previous algorithm in [10], this new pro-

cedure avoids additional refinement and expensive sorting by constructing a valid hierarchy directly.

6.1 Sufficient condition

A hierarchy of patches π^ℓ and spaces \mathbb{V}^ℓ , for $\ell = 1, \dots, N$, will be called *feasible* if the corresponding patchwork spline space can be equipped with a DPB-spline basis. Therefore, in order to analyze whether a given hierarchy is feasible, we have to check if NNC, IPC and SIC are satisfied for all patches and corresponding spline spaces. Verifying the latter two assumptions might be expensive since it requires us to go through all patch B-splines. However, for certain types of patches we can formulate conditions for IPC and SIC in the bivariate case, i.e., $d = 2$, that analyze only the boundary of a patch.

We define a *lower level boundary component* (LLBC) of a patch π^ℓ as a connected component of

$$\pi^k \cap \pi^\ell \neq \emptyset, \quad k < \ell.$$

Clearly, *IPC and SIC are satisfied for all patches with at most one LLBC.*

In addition to this simple observation, we present a necessary and sufficient condition for a certain class of patches. A *fat* patch π^ℓ is the union of mutually disjoint boxes composed of $p_1 \times p_2$ cells in Z^ℓ , where adjacent boxes share either a horizontal or a vertical boundary segment of p_1/p_2 knot spans, see Fig. 11. We consider single LLBCs of π^ℓ and connected components of I^ℓ . These parts of the boundary are denoted as *critical boundary components* if they are enclosed by LLBC(s) at both ends.

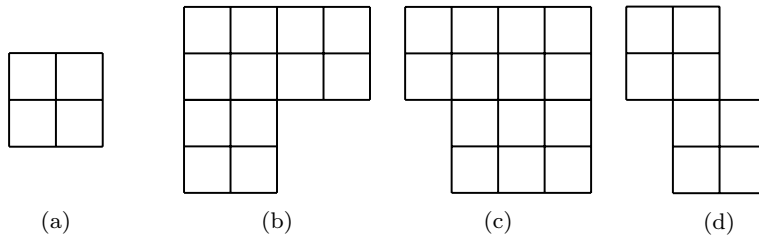


Fig. 11: Two fat patches (a) and (b) for $\mathbf{p} = (2, 2)$. The patch shown in (c) is not a fat patch, since not all disjoint boxes are composed of 2×2 cells and (d) is not a fat patch, since the shared segment between the north-western and the south-eastern boxes consisting of 2×2 cells is too short.

Corollary 2 *IPC and SIC are satisfied for a fat patch π^ℓ if and only if the width or the height of each critical component δ equals at least p_1 or p_2 knot spans with respect to \mathbb{V}^ℓ .*

Proof First, we show that the condition on the critical components is sufficient. The intersection $\text{supp}\beta^\ell \cap \partial\pi^\ell$, for $\beta^\ell \in B^\ell$ is either empty, a horizontal or vertical line segment that is $p_1 + 1$ or $p_2 + 1$ knot spans long with respect to \mathbb{V}^ℓ or a polygon composed of a horizontal and vertical line segment with a maximum length of p_1 and p_2 knot spans, respectively. Therefore, if a patch B-spline β^ℓ intersects two LLBCs of π^ℓ , γ_1 and γ_2 , then it holds that $\text{supp}\beta^\ell \cap \gamma_1 \cap \gamma_2 \neq \emptyset$. This implies IPC and SIC for π^ℓ .

Second, we prove that the condition is also necessary for IPC and SIC. We assume that there exists a critical boundary component δ that is joined to the LLBCs $\gamma_k \subseteq \pi^k$ and $\gamma_m \subseteq \pi^m$ at each end and does not meet the required assumption. Consequently, there exists a patch B-spline $\beta^\ell \in B^\ell$ such that

$$\text{supp}\beta^\ell \cap \gamma_k \neq \emptyset \quad \text{and} \quad \text{supp}\beta^\ell \cap \gamma_m \neq \emptyset.$$

If $k = m$ then SIC is not fulfilled. For $k \neq m$ IPC can be only satisfied if there is another LLBC γ' of π^k or π^m such that $\text{supp}\beta^\ell \cap \gamma_m \cap \gamma' \neq \emptyset$ or $\text{supp}\beta^\ell \cap \gamma_k \cap \gamma' \neq \emptyset$, respectively. However, then SIC is violated either for level k or m . \square

6.2 Macro elements

We consider bivariate tensor-product spline spaces of fixed degree $\mathbf{p} = (p_1, p_2)$ defined by uniform knot vectors obtained by performing r_i -times p_i -adic refinement in i -th direction, $i = 1, 2$. To be more precise, the spline space

$$\mathbb{S}^{\mathbf{r}} = \mathbb{S}^{(r_1, r_2)}$$

possesses the knot vector

$$(0, \dots, 0, \frac{1}{(p_i)^{r_i}}, \dots, \frac{(p_i)^{r_i} - 1}{(p_i)^{r_i}}, 1, \dots, 1),$$

in the i -th coordinate direction. These spline spaces are collected in a set, which we denote by \mathfrak{S} . A local spline space \mathbb{V}^ℓ is then defined as the restriction of a tensor-product spline space $\hat{\mathbb{V}}^\ell \in \mathfrak{S}$ to the corresponding patch. Consequently, there is a function

$$\mathbf{r} : \{1, \dots, N\} \rightarrow \mathbb{N} \times \mathbb{N}$$

such that $\hat{\mathbb{V}}^\ell = \mathbb{S}^{\mathbf{r}(\ell)}$ and

$$\mathbb{V}^\ell = \mathbb{S}^{\mathbf{r}(\ell)}|_{\pi^\ell}.$$

The knot lines of a spline space $\mathbb{S}^{\mathbf{r}}$ divide the domain into a set of cells $\hat{Z}^{\mathbf{r}}$. Hence, we obtain the local cell set

$$Z^\ell = \hat{Z}^{\mathbf{r}(\ell)}|_{\pi^\ell}.$$

We introduce a set of *macro elements* $\mathcal{M}^{\mathbf{r}}$, which contains the disjoint axis-aligned boxes consisting of $p_1 \times p_2$ cells in $\hat{Z}^{\mathbf{r}}$. To be more precise, the set $\mathcal{M}^{\mathbf{r}}$ contains the $p_1 \times p_2$ subgrids of $\hat{Z}^{\mathbf{r}}$ with lower left corners

$$\left(\frac{mp_1}{(p_1)^{r_1}}, \frac{np_2}{(p_2)^{r_2}} \right), \quad \text{for } m, n \in \mathbb{Z}.$$

6.3 Iterative refinement and its application to surface approximation

We consider an iterative refinement procedure consisting of several *refinement steps*. The input is a hierarchy where the patches are equal to the macro elements of an initial tensor-product spline space $\mathbb{S}^{\mathbf{r}}$. In each refinement step we add knots to the spline spaces of certain marked patches, thereby generating patches with finer spline spaces. A *refinement indicator* marks the cells that should be refined and a *direction indicator* specifies the refinement direction, i.e., whether we perform knot insertion in the first (or x_1 -) coordinate direction, second (or x_2 -) coordinate direction, or both. The concrete choice of these indicators depends on the application. For the case of surface approximation, it will be discussed below.

We refine such that the tensor-product spline spaces of neighboring patches are nested, which guarantees that NNC is fulfilled. As a consequence the refinement is not according to the direction indicator in some cases. Furthermore, all cells of a marked patch will be refined to the same spline space. Hence, a marked patch is replaced by at least p_1 , p_2 and $p_1 \times p_2$ patches, which are again macro elements, for refinement in x_1 -, x_2 - and both directions, respectively. More precisely we apply the following procedure:

- *Determining a refinement order:* We sort the marked macro elements $\mu \in \mathcal{M}^{\mathbf{r}(\ell)}$, for $\ell = 1, \dots, N$, lexicographically with respect to

$$(r_1(\ell) + r_2(\ell), r_2(\ell), \delta(\mu)).$$

The elements are then refined one by one in this order.

- *Refinement of the elements:* The corresponding spline space of an element $\mu \in \mathcal{M}^{\mathbf{r}(\ell)}$ is refined to a new spline space $\mathbb{V}^{\mathbf{r}(k)}$ that satisfies

$$(i) \quad r_i(k) \geq r_i(\ell), \quad \text{for } i = 1, 2,$$

- (ii) $\mathbb{S}^{\mathbf{r}(k)}$ is nested with the current spline spaces of neighboring patches,
and

$$(iii) |r_1(k) - r_2(k)| \leq 3.$$

Note that the property (iii) controls the aspect ratio of the elements. If refinement according to the direction indicator does not result in a space that fulfills these properties then we choose the smallest $\mathbf{r}(k)$ with respect to the lexicographical ordering $(r_1 + r_2, r_2)$ that satisfies them.

- *Final ordering:* We sort all macro elements lexicographically with respect to $(r_1 + r_2, r_2)$ and apply the selection mechanism.

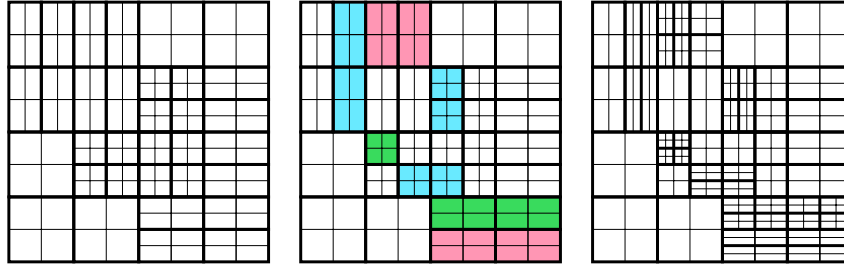


Fig. 12: Example 6 – Illustration of one refinement step.

Example 6 We consider the hierarchy in Fig. 12 on the left for $\mathbf{p} = (2, 2)$. The first five patches (nos. 1-5, south-west and north-east) are macro elements of the spline space $\mathbb{S}^{(3,3)}$, followed by eight macro elements (nos. 6-13, north-west) from $\mathcal{M}^{(4,3)}$ and eight elements (nos. 14-21, south-east) from $\mathcal{M}^{(3,4)}$. The remaining 12 patches (nos. 22-33, center) are elements of $\mathcal{M}^{(4,4)}$. Within each group of macro elements the chosen ordering does not affect the outcome of the algorithm in this case. The refinement and direction indicators mark certain patches for refinement as illustrated in the middle picture. Blue, red and green cells are marked for refinement in x_1 -, x_2 - and both directions, respectively. The image on the right shows the resulting mesh after the corresponding knot (local) insertion. Note that the macro element with lower left corner $(\frac{1}{4}, \frac{3}{4})$ is marked for refinement in x_2 -direction, which would result in non-nested spaces of neighboring patches. Therefore, we refine this patch in both directions instead. \diamond

A hierarchy that is constructed by this refinement procedure is feasible for DPB-splines. NNC is satisfied by the definition of the refinement algorithm. Moreover, all patches are boxes of size $p_1 \times p_2$ and according to the refinement mechanism, a patch shares an entire edge of its boundary either with a single patch of lower level or several patches of higher levels. Therefore, Corollary 2 guarantees that IPC and SIC are satisfied for all levels.

Furthermore, the so-constructed hierarchies also admit (T)PB-spline bases. Since all patches are aligned with the knot lines of the corresponding spline spaces CBA is satisfied. Moreover, the tensor-product basis functions $\hat{\beta}^\ell$ that

do not vanish on the corresponding patch π^ℓ intersect only with neighboring patches of lower level or higher level patches where the corresponding spline space is a superspace of \hat{V}^ℓ . This implies that FSC is satisfied.

The remainder of this section presents some details concerning the indicators used to perform *surface approximation*. More precisely, we use the refinement procedure in an iterative algorithm for approximating data with a DPB-spline surface by a standard regularized least-squares fitting, cf. [26]. The algorithm stops if the error does not exceed a user-defined threshold ε in a certain percentage of data points (usually between 95% and 99%) or the numbers of degrees of freedom or iteration steps exceed a predefined maximum. The *refinement algorithm* is guided by the following indicators:

- *Refinement indicator*: We mark all patches that contain points with an error exceeding a certain threshold.
- *Direction indicator*: The desired refinement direction for the marked elements is determined by a local-fitting method, see [10]. The direction indicator $\delta(\mu)$ takes the values 1, 2 or 3 for refinement in x_1 -, x_2 - and (x_1, x_2) -direction, respectively.

Example 7 We approximate the data set of Example 6 in [10] by biquadratic splines, i.e., $\mathbf{p} = (2, 2)$, and compare the hierarchies obtained from the macro element refinement (MER) and the original, simple patch refinement (SPR) algorithm presented in [10].

For both algorithms we choose the initial spline space $\mathbb{S}^{(3,3)}$, thus we obtain 4×4 initial macro elements/patches for MER. For SPR, the initial number of patches is user-defined and we decide to start from a single patch. The regularized least-squares fitting is solved with smoothness parameter $\lambda = 1e - 7$ and the iteration stops if the error in $\geq 98\%$ of the points is lower or equal to the threshold $\varepsilon = 1e - 4$. Fig. 13 depicts the resulting surface (note that the surfaces are visually identical for both algorithms and therefore we display only one of them) and meshes of both algorithms. Table 2 presents the number of degrees of freedom, some error statistics and computation times for both methods in rows 1 and 4, respectively. We observe that MER achieves a similar good result with fewer degrees of freedom than SPR. Furthermore, the sorting and possible additional refinement that is necessary for generating a feasible hierarchy in SPR is not required by MER, which is reflected in the lower computational times. The more patches are present in a hierarchy the more pronounced the difference becomes.

Moreover, we observed that SPR is very sensitive to the choice of the initial setting. If we choose the same initial spline space but start from four patches we obtain significantly worse results, see Table 2, second row. Therefore, in order to obtain good results in terms of number of degrees of freedom and computation time it is crucial to find a suitable initial setting for SPR. In contrast to this, the initial setting for MER is defined by the initial spline space only. We obtained nearly equivalent results for sufficiently coarse initial layouts, see row 3 and 5 of Table 2. \diamond

	no. of dofs	% of dofs	max. error	avg. error	total time
SPR – 1 patch	13,579	100%	$6.9e-4$	$2.24e-5$	8min 34sec
SPR – 4 patches	21,607	159%	$1e-3$	$2.28e-5$	1h 8min
MER – (2, 2)	9,732	71.7%	$6.4e-4$	$2.44e-5$	5min 46sec
MER – (3, 3)	9,732	71.7%	$6.4e-4$	$2.44e-5$	5min 40sec
MER – (4, 4)	9,732	71.7%	$6.4e-4$	$2.44e-5$	4min 52sec

Table 2: Example 7

Example 8 We reconstruct a real-world aircraft engine blade from $\approx 300,000$ data points, which were obtained by optical scanning. Many industrial applications require C^2 -smooth surfaces and thus, the data set is approximated by bicubic splines. We set $\lambda = 5d - 7$, $\varepsilon = 2d - 5$ and stop the iteration if $\geq 95\%$ of the data points are below the threshold. Again we compare the results of the SPR and MER algorithm, see Fig. 14 and 15 for images of the geometry and the meshes and Table 3 for statistics.

The SPR algorithm uses dyadic knot refinement and starts from the initial hierarchy consisting of 8 patches with initial spline spaces defined by the periodic knot vectors

$$\left(-\frac{3}{32}, -\frac{2}{32}, -\frac{1}{32}, 0, \frac{1}{32}, \dots, \frac{31}{32}, 1, \frac{33}{32}, \frac{34}{32}, \frac{35}{32}\right)$$

in both directions. The resulting mesh from the iterative fitting process is depicted in Fig. 15 (left) and additional information is given in the first row of Table 3. Changing the initial setting for SPR again leads to a drastically different result, see row 2 of Table 3.

For MER we start from the initial spline space $\mathbb{S}^{(3,3)}$ with periodic knot vectors and perform triadic knot refinement. The resulting mesh is depicted in Fig. 15 on the right. As before, the algorithm yields a result with fewer degrees of freedom and less computation time but comparable errors, see fourth row of Table 3. Furthermore, MER leads to a surface with a better visual quality compared to the result obtained by SPR, see Fig. 14. The SPR based surface (center) possesses oscillations that are not present or less pronounced in the MER based surface (right). Choosing the initial spline spaces $\mathbb{S}^{(2,2)}$ and $\mathbb{S}^{(4,4)}$ again leads to similar results, see rows 3 and 5 of Table 3. Although the numbers of degrees of freedom vary, all three initial settings need similar computation time and lead to similar approximation errors. \diamond

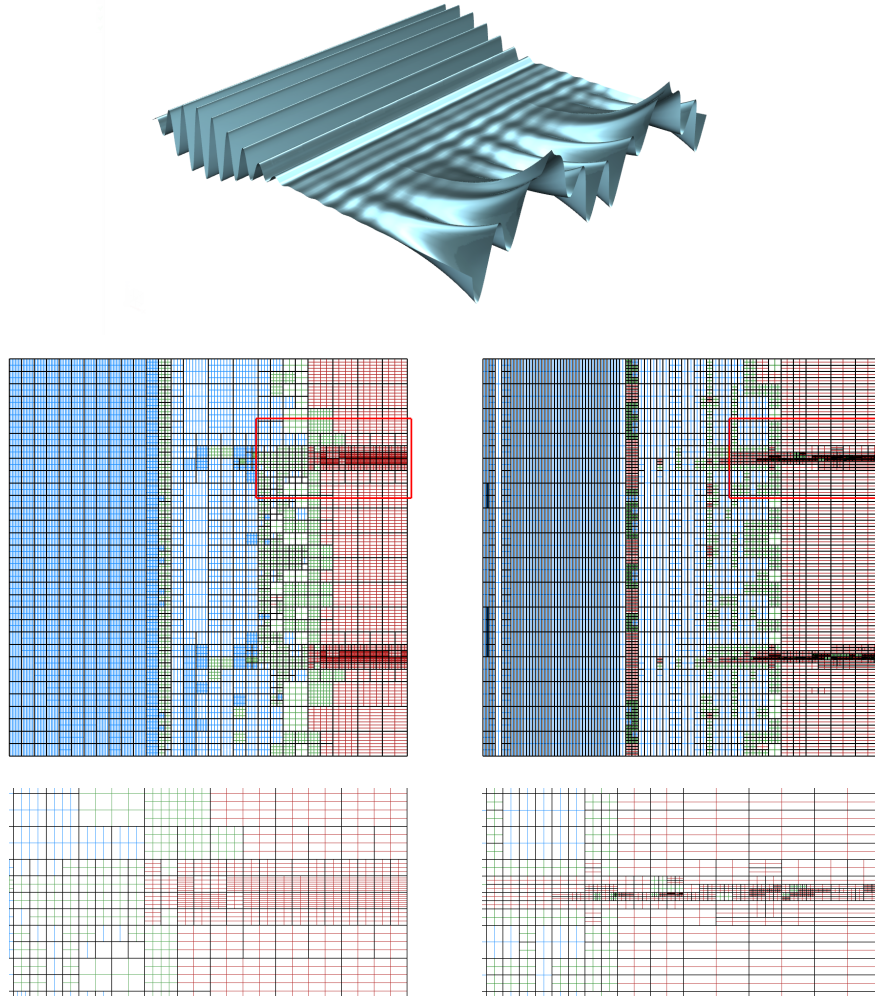


Fig. 13: Example 7 – Approximated surface (top) and corresponding meshes for SPR (left) and MER (right). Patch boundaries are black. The knot lines of a spline space $\mathbb{S}^{(r_1, r_2)}$ are colored according to the dominant refinement direction, from blue ($r_1 > r_2$) via green ($r_1 = r_2$) to red ($r_1 < r_2$).

7 Conclusion

The definition of a TPB-spline basis requires a strong nestedness assumption, which limits the choice of possible refinement strategies. The new construction of DPB-splines, which was presented in this paper, substantially increases the flexibility for anisotropic refinement. The use of locally defined,

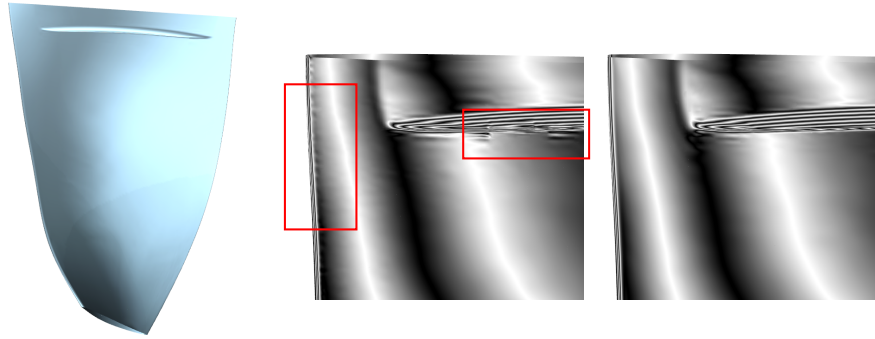


Fig. 14: Example 8 – Approximated surface (left) and reflection line analysis for SPR (middle) and MER (right).

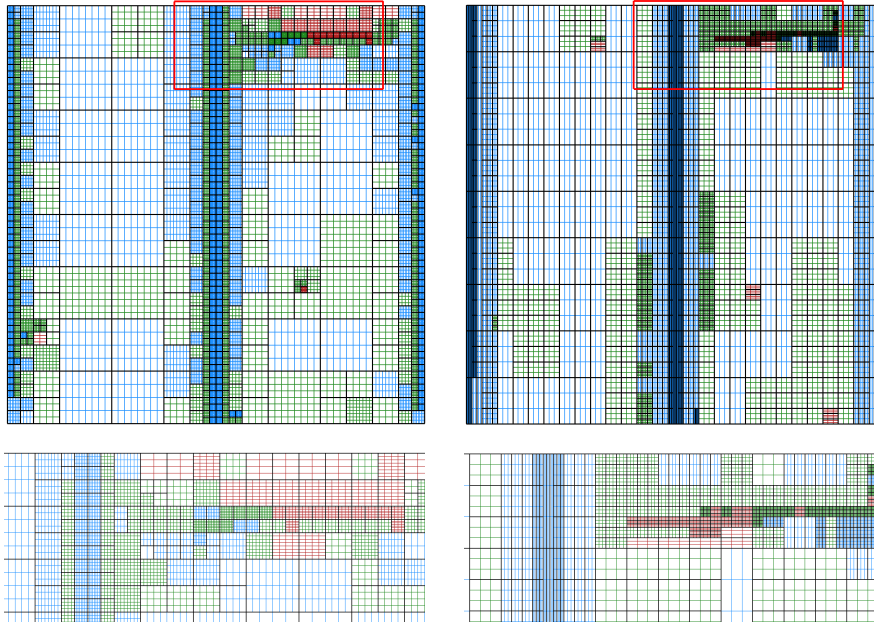


Fig. 15: Example 8 – Meshes for SPR (left) and MER (right).

	no. of dofs	% of dofs	max. error	avg. error	total time
SPR – 16 patches	19,823	100%	$5.0e-5$	$3.32e-6$	17min 38sec
SPR – 64 patches	31,184	157.3%	$1.1e-3$	$3.51e-6$	54min 40sec
MER – (2, 2)	9,774	49.3%	$5.6e-5$	$3.84e-6$	11min 47sec
MER – (3, 3)	13,284	67%	$5.6e-5$	$3.33e-6$	10min 20sec
MER – (4, 4)	24,498	123.6%	$5.6e-5$	$3.01e-6$	14min

Table 3: Example 8

decoupled basis functions enables the definition of a basis under three assumptions (NNC, IPC and SIC) that affect only the direct neighborhood of a patch. In particular, only the spaces associated with neighboring patches have to be nested. Furthermore, for a certain class of patches we identified a particularly simple sufficient condition for IPC and SIC.

The DPB-splines possess the required order of smoothness, they span the patchwork spline space, form a non-negative partition of unity and preserve the coefficients of the local B-spline representations. Moreover, the DPB-splines are algebraically complete, i.e., the patchwork spline space is equal to the full spline space. This property is not necessarily satisfied for the (T)PB-splines. Although there exist some hierarchies that are valid for TPB-splines but cannot be equipped with a DPB-spline basis, this set is rather small compared to the hierarchies that are feasible for DPB-splines and do not allow the definition of a TPB-spline basis.

Finally, the definition of DPB-splines inspired us to introduce a new refinement algorithm for least-squares fitting. The resulting hierarchies admit a PB-, TPB- and DPB-spline basis. Furthermore, this macro element-based refinement offers the significant advantage that a feasible hierarchy is automatically generated without the additional sorting and refinement that is required for the previous SPR algorithm presented in [10]. This enabled us to reduce the computation time and the number of degrees of freedom compared to SPR, while preserving the high quality of the results.

Acknowledgment

The financial support of the FWF (NFN S117 “Geometry + Simulation” and Doctoral Program W1214 “Computational Mathematics”) and of the ERC (GA no. 694515) is gratefully acknowledged. Special thanks go to the geometry department at MTU Aero Engines for providing the data of the turbine blade example.

References

1. H.R. Atri and S. Shojaee. Truncated hierarchical B-splines in isogeometric analysis of thin shell structures. *Steel Compos. Struct.*, 26(2):171–182, 2018.
2. P. B. Bornemann and F. Cirak. A subdivision-based implementation of the hierarchical B-spline finite element method. *Comput. Meth. Appl. Mech. Engrg.*, 253:584–598, 2013.
3. C. Bracco, A. Buffa, C. Giannelli, and R. Vázquez. Adaptive isogeometric methods with hierarchical splines: An overview. *Discrete and Continuous Dynamical Systems- Series A*, 39(1):241–262, 2019.

4. C. Bracco, C. Giannelli, D. Großmann, and A. Sestini. Adaptive fitting with THB-splines: Error analysis and industrial applications. *Comput. Aided Geom. Design*, 62:239 – 252, 2018.
5. A. Buffa and C. Giannelli. Adaptive isogeometric methods with hierarchical splines: error estimator and convergence. *Math. Meth. Appl. Sc.*, 26:1–25, 2016.
6. L. Chen and R. de Borst. Adaptive refinement of hierarchical T-splines. *Comput. Meth. Appl. Mech. Engrg.*, 337:220–245, 2018.
7. L. Chen and R. de Borst. Locally refined T-splines. *Int. J. Numer. Meth. in Engrg.*, 114(6):637–659, 2018.
8. L. Beirão da Veiga, A. Buffa, D. Cho, and G. Sangalli. Analysis-suitable T-splines are dual-compatible. *Comput. Meth. Appl. Mech. Engrg.*, 249–252:42–51, 2012.
9. T. Dokken, T. Lyche, and K. F. Pettersen. Polynomial splines over locally refined box-partitions. *Comput. Aided Geom. Design*, 30:331–356, 2013.
10. N. Engleitner and B. Jüttler. Patchwork B-spline refinement. *Comput. Aided Design*, 90:168–179, 2017.
11. N. Engleitner and B. Jüttler. Lofting with patchwork B-splines. In C. Giannelli and H. Speleers, editors, *Advanced Methods for Geometric Modeling and Numerical Simulation*, volume 35 of *INdAM Series*, pages 77–98. Springer, 2019.
12. N. Engleitner, B. Jüttler, and U. Zore. Partially nested hierarchical refinement of bivariate tensor-product splines with highest order smoothness. In M. Floater et al., editors, *Mathematical Methods for Curves and Surfaces*, Lecture Notes in Computer Science, pages 126–144. Springer, 2017.
13. E. J. Evans, M. A. Scott, X. Li, and D. C. Thomas. Hierarchical T-splines: analysis-suitability, Bézier extraction, and application as an adaptive basis for isogeometric analysis. *Comput. Meth. Appl. Mech. Engrg.*, 284:1–20, 2015.
14. G. Farin, J. Hoschek, and M.-S. Kim, editors. *Handbook of Computer Aided Geometric Design*. Elsevier, 2002.
15. D. R. Forsey and R. H. Bartels. Hierarchical B-spline refinement. *Comput. Graphics*, 22:205–212, 1988.
16. E.M. Garau and R. Vázquez. Algorithms for the implementation of adaptive isogeometric methods using hierarchical B-splines. *Applied Numerical Mathematics*, 123:58–87, 2018.
17. C. Giannelli, B. Jüttler, S.K. Kleiss, A. Mantzaflaris, B. Simeon, and J. Špoh. THB-splines: An effective mathematical technology for adaptive refinement in geometric design and isogeometric analysis. *Comput. Meth. Appl. Mech. Engrg.*, 299:337–365, 2016.
18. C. Giannelli, B. Jüttler, and H. Speleers. THB-splines: The truncated basis for hierarchical splines. *Comput. Aided Geom. Design*, 29:485–498, 2012.
19. C. Giannelli, B. Jüttler, and H. Speleers. Strongly stable bases for adaptively refined multilevel spline spaces. *Adv. Comput. Math.*, 40(2):459–490, 2014.
20. C. Giannelli, T. Kanduč, F. Pelosi, and H. Speleers. An immersed-isogeometric model: Application to linear elasticity and implementation with THBox-splines. *J. Comput. Appl. Math.*, 349:410–423, 2019.
21. A. Giust, B. Jüttler, and A. Mantzaflaris. Local (T)HB-spline projectors via restricted hierarchical spline fitting. *Comput. Aided Geom. Design*, 80:101865, 2020.
22. G. Greiner and K. Hormann. Interpolating and approximating scattered 3D-data with hierarchical tensor product B-splines. In A. Le Méhauté, C. Rabut, and L.L. Schumaker, editors, *Surface Fitting and Multiresolution Methods*, pages 163–172. Vanderbilt University Press, Nashville, TN, 1997.
23. T. Kanduč, C. Giannelli, F. Pelosi, and H. Speleers. Adaptive isogeometric analysis with hierarchical box splines. *Comput. Meth. Appl. Mech. Engrg.*, 316:817–838, 2017.
24. H. Kang, F. Chen, and J. Deng. Hierarchical B-splines on regular triangular partitions. *Graph. Models*, 76(5):289–300, 2014.

25. H. Kang, J. Xu, F. Chen, and J. Deng. A new basis for PHT-splines. *Graphical Models*, 82:149–159, 2015.
26. G. Kiss, C. Giannelli, U. Zore, B. Jüttler, D. Großmann, and J. Barner. Adaptive CAD model (re-)construction with THB-splines. *Graph. Models*, 76(5):273–288, 2014.
27. R. Kraft. *Adaptive und linear unabhängige Multilevel B-Splines und ihre Anwendungen*. PhD thesis, Univ. Stuttgart, 1998.
28. G. Kuru, C. Verhoosel, K. van der Zeeb, and E. van Brummelen. Goal-adaptive isogeometric analysis with hierarchical splines. *Comput. Meth. Appl. Mech. Engrg.*, 270:270–292, 2014.
29. X. Li, J. Deng, and F. Chen. Polynomial splines over general T-meshes. *Visual Comput.*, 26:277–286, 2010.
30. X. Li, J. Zheng, T. W. Sederberg, T. J. R. Hughes, and M. A. Scott. On linear independence of T-spline blending functions. *Comput. Aided Geom. Design*, 29:63–76, 2012.
31. D. Mokriš and B. Jüttler. TDHB-splines: The truncated decoupled basis of hierarchical tensor-product splines. *Comput. Aided Geom. Design*, 31(7–8):531–544, 2014.
32. D. Mokriš, B. Jüttler, and C. Giannelli. On the completeness of hierarchical tensor-product B-splines. *J. Comput. Appl. Math.*, 271:53–70, 2014.
33. P. Morgenstern and D. Peterseim. Analysis-suitable adaptive T-mesh refinement with linear complexity. *Comput. Aided Geom. Design*, 34:50–66, 2015.
34. D. Schillinger et al. An isogeometric design-through-analysis methodology based on adaptive hierarchical refinement of NURBS, immersed boundary methods, and T-spline CAD surfaces. *Comput. Meth. Appl. Mech. Engrg.*, 249–252:116–150, 2012.
35. T. W. Sederberg, J. Zheng, A. Bakenov, and A. Nasri. T-splines and T-NURCCS. *ACM Trans. Graphics*, 22:477–484, 2003.
36. H. Speleers. Hierarchical spline spaces: quasi-interpolants and local approximation estimates. *Adv. Comp. Math.*, 43:235–255, 2017.
37. H. Speleers, P. Dierckx, and S. Vandewalle. Quasi-hierarchical Powell-Sabin B-splines. *Comput. Aided Geom. Design*, 26:174–191, 2009.
38. H. Speleers and C. Manni. Effortless quasi-interpolation in hierarchical spaces. *Numer. Math.*, 132:155–184, 2016.
39. X. Wei, Y. Zhang, T. J. R. Hughes, and M. A. Scott. Extended truncated hierarchical Catmull-Clark subdivision. *Comput. Meth. Appl. Mech. Engrg.*, 299:316–336, 2016.
40. A. Yvart, S. Hahmann, and G.-P. Bonneau. Hierarchical triangular splines. *ACM Trans. Graphics*, 24:1374–1391, 2005.
41. J. Zhang and X. Li. Local refinement for analysis-suitable++ T-splines. *Comput. Meth. Appl. Mech. Engrg.*, 342:32–45, 2018.
42. U. Zore and B. Jüttler. Adaptively refined multilevel spline spaces from generating systems. *Comput. Aided Geom. Design*, 31:545–566, 2014.
43. U. Zore, B. Jüttler, and J. Kosinka. On the linear independence of truncated hierarchical generating systems. *J. Comput. Appl. Math.*, 306:200–216, 2016.